

## Reply to Reviewers

We thank the reviewers for their comments and suggestions on this manuscript. We present some general comments first and then address specific comments below. We were unaware of the Cabre et al. (2015) paper at submission, but now compare many aspects of our results with this work in the revised manuscript. Both Cabre et al. (2015) and Bopp et al. (2013) examined the same group of CMIP 5 ocean biogeochemical models as this work. We feel this work strongly complements these two excellent papers. Bopp et al. (2013; and to some extent Cabre et al., 2015) focus more on model-mean responses, and model trends normalized to 1990s values, emphasizing similarities in the model responses to climate change. Cabre et al. (2015) also include detailed analysis of key ocean biomes and changes between the beginning and end of the century under RCP 8.5. We also reference an additional multi-model analysis of the response of NPP to climate change by Laufkötter et al. (2015) in the revised manuscript.

The emphasis in our work is partly on illustrating the wide spread across models for key biogeochemical and physical metrics from the current era, and understanding how that impacts the responses to climate change. Secondly, we wanted to identify, at the global scale, what drives the climate change responses in NPP and sinking export production. The CMIP5 ocean biogeochemical models are an increasingly important component of our climate projections (i.e. Randerson et al., 2015). Considering the vast resources committed (both human and computational), and the societal importance of predicting how the Earth system will respond to climate change, we agree with Reviewer #1 that there needs to be much more study of these models, from different perspectives. CMIP5 marks the first time ocean biogeochemistry has been included in most of these Earth System Models, and detailed documentation of model performance and results is necessary. Quantifying each model's performance relative to current-era observations, also allows for objective evaluation over time as to whether these models are improving. The target audience for this work includes the oceanographic and broader climate communities.

There are a number of new results and perspectives presented here, that are not found in previous works. Both reviewers note our novel finding that the models with the strongest positive biases in stratification for the 1990s, also show the strongest increases in stratification and the largest decreases in export production and NPP with climate change.

We present times series of the absolute values (not normalized to each model mean for some period) of key physical and biogeochemical variables, illustrating the wide inter-model spread (and the poor comparison to observed values) in surface nutrient

concentrations (Figure 3), productivity and export (Figure 5), and sea surface temperature, salinity, and surface stratification (Figure 1). We also show 2-D maps of surface nitrate for the 1990s from all the models compared with the World Ocean Atlas (Figure S3). These figures allow readers to examine each model's fidelity to observations for the current era, and illustrate the large spread across the models. No plots like these have appeared in prior works. Similarly, we show the 2-D spatial patterns for diatom contribution to NPP and the particle export ratio (Figures 8 and 10), and the 2d patterns of how these change with climate (Figures 9 and 12). This complements the biome by biome analysis of by Cabre et al. (2015), and illustrates the links between plankton community composition and export efficiency.

We emphasize comparing the biogeochemical variables with stratification as a key driver, as this metric better captures high-latitude, salinity-driven climate impacts than SST alone. We also present 2D plots showing where warming and salinity changes dominate the stratification changes for each model (Figure S2), and show the spatial patterns of stratification change by the end of the century (Figure 2). Previous works have focused more on the model-mean response and areas of model agreement, we highlight the similarities and the disagreements across the models in the spatial patterns of stratification change and in the dominant process driving stratification changes (temperature vs. salinity).

Our analysis of the impacts of changing stratification on biogeochemical variables utilizes the full time series from each model, rather than just comparing the beginning and end of the century. We examine how stratification impacts biogeochemistry, phytoplankton community structure, and export efficiency using 150 data points for each model over the period 1851-2100 (Figure 10), rather than just two points per model, based on beginning and end of century, decadal time-scale means. Thus our regressions and illustrations of the similarities and differences across the models are more robust, and are more easily visualized in the plots for each model, than in previous analyses (Figure 10).

Anonymous Referee #1

Received and published: 29 September 2015

General comment

The paper by Fu et al. presents changes in marine productivity under a global warming scenario simulated by CMIP5 models. I think this work is meaningful because comparison of marine ecosystem variables across CMIP5 models is still limited. Their indication that models having larger biases in stratification in contemporary period show stronger stratification in future climate is important. They pointed also out that representation of community composition in

models is an important factor to determine productivity response to climate change, which can be a motivation to represent marine ecosystem dynamics more realistically in CMIP models. Their analysis, however, looks crude in some aspects, and additional investigations are required before publishing.

**We thank the reviewer for the comments. We agree that more comparative studies across the CMIP5 models are warranted.**

Specific comments

1. Controlling factors other than stratification

In this paper, the authors focused mainly on relationship between marine biogeochemical variables and stratification. Although high correlations between these variables (Fig. 10) highlight an importance of stratification, other factors, changes in light availability and temperature increase, can contribute to the simulated production changes. In p. 12869 L. 13-16, the authors concluded that increased stratification and nutrient stress are the dominant control on the production change in comparison with changes in light and temperature. There is, however, no analysis supporting this argument.

**In our discussion, we focus on the global scale response, where increasing stratification is the dominant factor leading to decreasing NPP and export. We also acknowledge that temperature and light can also impact the response to climate change, particularly in the polar-regions. We will clarify and expand this discussion section in a revised manuscript. In fact, the three limiting factors, stratification, light and temperature are not independent. Stratification, as a function of temperature and salinity, is closely related to MLD and thermocline depth. Stratification also affects nutrient supply and light availability. At high latitudes, light can often be a limiting factor for phytoplankton growth. The changes in light are largely associated with ice retreat and changes in MLD. Enhanced stratification and shoaled MLD increase light availability and can result in higher production (Sarmiento et al. 2004; Bopp et al. 2005; Doney 2006; Steinacher et al. 2010). However, increased stratification leads to reduced nutrient supply and PP in many regions, which dominates the global response (Bopp et al. 2005; Cabre et al., 2015). We show that the stratification metric captures both the temperature-driven changes that dominate at low to mid-latitudes, and the salinity-driven changes at higher latitudes. On a global scale, over the full 1850-2100 time period, the changes in NPP and EP are more highly correlated with the changes in**

stratification, than with the changes in SST ( $r^2$  0.72 for stratification-NPP and 0.66 for SST-NPP). The relationship between the change of PAR and NPP was shown to be significant only in the sea-ice covered area of south hemisphere by Cabre et al. (2015), with a similar result found by Laufkötter et al. (2015). We note these findings in the introduction section of the revised ms and do not see the need to replicate these analyses a third time here.

## 2. Spatial pattern of production change

The authors mainly discuss changes in globally averaged variables. Discussions for changes in spatial patterns can strengthen their argument. For example, although they argue that stratification is the main driver decreasing productivity, the spatial patterns of changes in stratification (Fig. 4) and NPP by diatoms (Fig. 12) are quite different. How do the authors explain this discrepancy? From my view, there are some characteristic responses in the spatial pattern of NPP change among models. In the complicated models (GFDLs, IPSLs and CESM), the responses of NPP by diatoms show decrease in the northern high latitudes, small increase in tropics and subtropics, and modest increase in the Southern Ocean (Fig. 12). In the simpler models, on the other hand, show decrease in the northern high latitudes and increase in tropics and subtropics. What controls such different response?

**One key factor driving the different response we document is the stronger declines in surface nutrients and increasing nutrient stress in the high northern latitudes, and the resulting larger shifts in plankton community composition. Some of the regions with the strongest increases in stratification (like the western tropical Pacific) have only a small contribution of diatoms in the current era, so large declines are not possible. This factor largely explains the differences between Figure 4 and 12. Increasing stratification does reduce nutrient availability for the small phytoplankton as well, but the varying degrees of nutrient stress drives the community shifts. Thus, the response of the %NPP by diatoms depends on several factors, including whether they were a small or large component of the community initially. As the reviewer notes, and we address in the paper, the largest decreases are seen in areas with high diatom production initially and large increases in stratification, particularly in the Northern Hemisphere. In the Southern Ocean, the winds that drive upwelling strengthen in these models, influencing iron supply, a point we will make more fully in the revised manuscript. Cabre et al. (2015) also address the asymmetry in the biogeochemical response to climate change. We added text in the discussion to bring relevant previous work (i.e. Marinov et al., 2013; Moore et al., 2013, Cabre et al., 2015; etc..).**

Minor comments and questions

1. Add units (kg/m<sup>3</sup>?) in p. 12886 Fig. 4.

**The unit was added.**

2. What is the definition of the particle export ratio?

**Particle export ratio is defined as the sinking production flux out of the euphotic zone to net primary production in this work, based on Dunne et al. (2007). The broader term, export ratio, should also include the export of dissolved organic matter, which we do not address here. We clarified this in the revised manuscript.**

3. p. 12897 Fig. 15 Are these regression slopes statistically significant? If so, please write it, and also describe what significant level is used.

**The slopes are plotted when the correlation is significant at >95% level. We note this in the revised manuscript.**

Anonymous Referee #2

Received and published: 2 November 2015

The paper compares 9 CMIP5 ESM in terms of NPP, EP, surface nutrients, and stratification. There is some very detailed comparison of these various fields. Several recent studies have done similar comparisons (e.g. Bopp et al 2013, Cabre et al 2013) and there have been numerous studies that have considered projected NPP, EP and nutrient changes as function of warming and stratification (e.g. Bopp et al 2001, Bopp et al 2005, Dutkiewicz et al 2013, Marinov et al., 2010; Taucher and Oschlies et al 2012), and several that have also considered changes in phytoplankton community structure (e.g. Bopp et al 2005, Dutkiewicz et al, 2013, Cabre et al, 2015). Thus almost everything this manuscript addresses has been discussed before. This manuscript has some more specific numbers for the variability between models (though similar comparison also have noted this variability though the numbers are a bit different depending which models they included). I struggled therefore to find something new (and useful) in this manuscript. The pieces I did find were:

1) models with largest increases in stratification have strongest changes in NPP and EP (Bopp et al, 2013 had something similar but using changes in SST rather than stratification).

2) models with largest increases in stratification also showed the largest biases for the contemporary period (suggesting potential overestimating climate impacts).

3) Models with dynamic phytoplankton communities show larger decline in EP than NPP (but this could be anticipated any of the previous work that has suggested shifts from large to small phytoplankton and if they parameterize large as having larger impact on export).

**We agree that these are three important results, but as noted previously, there is much more new and novel in our paper than these three items.**

The second point is potentially exciting. A careful analysis of the differences in stratification helped identify this. I recommend rewriting a significantly shortened paper which highlights this aspect over a long-winded summary of the detailed comparisons. For instance, the current discussion makes no mention of the point on this stratification/bias issue, but includes a long list of numbers (not particularly useful as it depends on which set of models one looks at – see e.g. Bopp et al 2013, Cabre et al 2015) and focuses on things that have already been addressed elsewhere in the literature (NPP varies more than EP – Bopp et al 2013; shifts in community structure – Bopp et al 2005 (and many others)).

**The Bopp et al. (2013) paper mainly focuses on temperature-related factors as driving the different patterns of NPP response to climate change. Cabre et al. (2015) discuss community composition as a relevant factor, we not extensively cite this paper. The fact that community structure, and its implementation in the models, largely determines the NPP response to climate change has not been emphasized previously. The relationship between community composition and export efficiency in these models is familiar to ocean biogeochemical modelers, but less so to the larger oceanographic community, and is likely completely unknown to the climate community.**

A long discussion about how CMIP5 models are far from perfect seems irrelevant in the face that several other studies have said similar things.

**Previous studies did not highlight the imperfections in the CMIP5 models in the same manner as this paper, but in fact downplayed these large differences by focusing on model-mean results and trends normalized to the mean 1990s values from each model. Both approaches have merit, and as mentioned above, we believe what is needed is more analysis of the CMIP5 models, not less. But our perspective is very different, in part, precisely to highlight the large inter-model differences. We show large variations in the simulated surface nutrients**

across the CMIP5 models (by a factor of ~1.5-2.5 for no<sub>3</sub>, po<sub>4</sub> and sio<sub>4</sub>; a factor of ~5 for dissolved iron). This has not been discussed in detail or illustrated in this manner previously. In the context of the large model spread, we tried to find robust connections between physics and biogeochemistry. The change of stratification was highlighted as a primary driver to NPP and EP changes throughout the multi-century simulations. On a global scale, we identified a closer relationship between stratification and NPP/EP changes over the period of 1850-2100, than with other factors such as SST or SSS changes across the models.

I suggest shorting to less figures and removal of details that can be referenced to other studies. Details of the nutrient changes I found somewhat less interesting – nutrient supply rate changes are what is important. I was convinced that there was useful information that came from this part of the analysis. This also applies to Fig 3.

**In an effort to shorten the paper, we have eliminated non-essential text and moved three of the figures to supplementary materials. We think it is important to include the figures showing the large spread in surface nutrient concentrations and NPP relative to the observations. These have not been included in prior studies and are of interest and value. It is insightful to see, for each model, the biases present for the current era, and as we show, it helps to interpret the varied responses to climate change. In this paper, we quantify the relations between stratification and biogeochemical variables over the entire time period of 1850-2100. Cabre et al (2015) examined the relations between variables across CMIP5 models by 100-year time-scale changes (difference between 2080–2099 and 1980–1999). Bopp et al. (2013) and largely followed a similar approaches. Both approaches have merit, but they are different analyses.**

Besides a much shorter paper, I suggest much greater care on the discussion which I found to delve into speculation and grandiose statement that I do not feel are supported by (or even relevant to) the paper. For instance:

Pg 12870: lines 10-20. I find this discussion potentially dangerous. I will agree that changes in EP is a better metric for climate impacts on carbon cycle; but disagree that it is best metric for “marine ecosystems” or food chains and fisheries. Community structure changes are also very important for marine systems and can potentially not be captured in EP. Additionally EP is possibly worse in parameterization than NPP in models. Before arguing this too fully it would be

worth looking at how each of the models determines EP (Martin curve, explicit particle sinking) and how they parameterize how much is exported relative to community structure.

**Our main point here was that the community shifts minimize the declines in NPP as export efficiency declines and regenerated production increases in the more complex models. This can be misleading if one only examines the NPP response, particularly in terms of climate feedbacks and the carbon cycle as suggested by the reviewer. We would argue that export production does have strong relevance for higher trophic levels, but perhaps this was worded too broadly in the original manuscript. We have modified the text to merely suggest export production as an additional key metric. We agree with the reviewer that improved representation of community structure is needed in this class of models, precisely to improve model predictions of export and export efficiency. Indeed this is one of our key conclusions, which we express more clearly in the revised manuscript.**

Could models have more similar changes in EP because they are all so crude in how they parameterize EP?

Since the models are so crude in parameterizing the complex processes involved in EP (role of bacteria, Archea etc etc): should EP be sold as a “best” metric for any impact of climate change? This goes back to my point (3) above.

**It is not the crudeness of the parameterization of the remineralization curve that gives the models a more similar response in EP, but simply the fact that over large enough time and space scales, the total EP must equal the input of new nutrients from circulation and mixing (plus other sources atmospheric, N fixation, etc..). Thus, as stratification increases and nutrient inputs decline, EP declines. To some extent, the prescribed remineralization curves have been optimized to match the observed global mean nutrient profiles. We argue that the levels of regenerated production vary substantially across the models, and that the regenerated production level is not constrained by the physics and nutrient input fluxes, but by the export efficiency built into each model.**

On a final note to the community at large: How much more useful (as opposed to “details” on models we know are flawed) information can be wrung out of CMIP5 comparisons?

**This comment has been addressed in previous sections.**



A. Cabre

[annanusca@gmail.com](mailto:annanusca@gmail.com)

Received and published: 17 August 2015

Please note that we already published a paper comparing global response of phytoplankton and PP over the 21st century in the entire suite of CMIP5 models

(<http://link.springer.com/article/10.1007/s00382-014-2374-3>). We discussed the primary production responses across models on a biome by biome basis and found many of the same patterns. It would be interesting to discuss how your new results fit our earlier findings.

**We thank the author for pointing this paper out. We made comparisons with the results from Cabre et al. (2015) in many places throughout the revised manuscript, with a total of 16 citations of this work. We have also added additional comparisons of our results with the highly relevant multi-model studies by Bopp et al. (2013) and Laufkötter et al. (2015).**

## References:

- Bopp, L., O. Aumont, P. Cadule, S. Alvain, and M. Gehlen, 2005: Response of diatoms distribution to global warming and potential implications: A global model study. *Geophysical Research Letters*, **32**.
- Bopp, L., and Coauthors, 2013: Multiple stressors of ocean ecosystems in the 21st century: projections with CMIP5 models. *Biogeosciences*, **10**, 6225-6245.
- Cabré, A., I. Marinov, R. Bernardello, and D. Bianchi, 2015: Oxygen minimum zones in the tropical Pacific across CMIP5 models: mean state differences and climate change trends. *Biogeosciences*, **12**, 5429-5454.
- Doney, S. C., 2006: Oceanography - Plankton in a warmer world. *Nature*, **444**, 695-696.
- Dunne, J. P., J. L. Sarmiento, and A. Gnanadesikan, 2007: A synthesis of global particle export from the surface ocean and cycling through the ocean interior and on the seafloor. *Global Biogeochemical Cycles*, **21**.
- Moore, J., K. Lindsay, S. Doney, M. Long, and K. Misumi, 2013: Marine Ecosystem Dynamics and Biogeochemical Cycling in the Community Earth System Model [CESM1(BGC)]: Comparison of the 1990s with the 2090s under the RCP4.5 and RCP8.5 Scenarios. *J Climate*, **26**, 9291-9312.
- Marinov, I., Doney, S. C., Lima, I. D., Lindsay, K., Moore, J. K., and Mahowald, N.: North–South asymmetry in the modeled phytoplankton community response to climate change over the 21st century, *Global Biogeochem. Cy.*, 27, GB004599, doi:10.1002/2013GB004599, 2013. 3734, 3736, 3759, 3761, 3762
- Randerson, J. T., and Coauthors, 2015: Multicentury changes in ocean and land contributions to the climate-carbon feedback. *Global Biogeochemical Cycles*, **29**, 744-759.
- Sarmiento, J. L., and Coauthors, 2004: Response of ocean ecosystems to climate warming. *Global Biogeochemical Cycles*, **18**.
- Steinacher, M., and Coauthors, 2010: Projected 21st century decrease in marine productivity: a multi-model analysis. *Biogeosciences*, **7**, 979-1005.

1  
2  
3  
4  
5  
6  
7  
8  
9  
10  
11  
12  
13  
14  
15  
16  
17

**Climate Change Impacts on Net Primary Production (NPP) and Export  
Production (EP) Regulated by Increasing Stratification and Phytoplankton  
Community Structure in [the](#) CMIP5 Models**

Weiwei Fu, James Randerson and J. Keith Moore

Department of Earth System Science, University of California, Irvine, California,  
USA, 92697

18 **Abstract**

19 We examine climate change impacts on net primary production (NPP) and  
20 export production (sinking particulate flux; EP) with simulations from nine Earth  
21 System Models (ESMs) performed in the framework of the fifth Coupled Model  
22 Inter-comparison Project (CMIP5). Global NPP and EP are reduced by the end of  
23 the century for the intense warming scenario of Representative Concentration  
24 Pathway (RCP) 8.5. Relative to the 1990s, NPP in the 2090s is reduced by 2.3-16%  
25 and EP by 7-18%. The models with the largest increases in stratification (and  
26 largest relative declines in NPP and EP) also show the largest positive biases in  
27 stratification for the contemporary period, suggesting some overestimation of  
28 climate change impacts on NPP and EP. All of the CMIP5 models show an  
29 increase in stratification in response to surface ocean warming and freshening,  
30 which is accompanied by decreases in surface nutrients, NPP, and EP.

31 There is considerable variability across the models in the magnitudes of NPP,  
32 EP, surface nutrient concentrations, and their perturbations by climate change.  
33 The negative response of NPP and EP to increasing stratification reflects  
34 primarily a bottom-up control, as upward nutrient flux declines at the global  
35 scale. Models with dynamic phytoplankton community structure show larger  
36 declines in EP than in NPP. This pattern is driven by phytoplankton community  
37 composition shifts, with reductions in productivity by large phytoplankton as  
38 smaller phytoplankton (which export less efficiently) are favored under the  
39 increasing nutrient stress. Thus, the projections of the NPP response to climate  
40 change are critically dependent on the simulated phytoplankton community  
41 structure, the efficiency of the biological pump, and the resulting levels of  
42 regenerated production, which vary widely across the models. Community  
43 structure is represented simply in the CMIP5 models, and should be expanded

Deleted: d considerably

Deleted: global

Deleted: reductions

Deleted: some potential

Deleted:

Deleted: that

Deleted: , and surface macronutrient concentrations.

Deleted: absolute

Deleted: these fluxes

Deleted: , indicating large model uncertainties

Deleted: increases

Deleted: nutrient flux to the euphotic zone declines

Deleted: a reduced percentage of NPP by

Deleted: under RCP 8.5,

Deleted: in the CMIP5 models

Deleted: (highly variable)

Deleted: .

Deleted: composition

Deleted: relatively

Deleted: , and

Deleted:

65 and improved to better capture the spatial patterns and changes in export  
66 efficiency that seem necessary for predicting climate change impacts on NPP.  
67

Deleted: the

Deleted: are

70 **1 Introduction**

71 Ocean net primary production (NPP) and particulate organic carbon export  
72 (EP) are key elements of marine biogeochemistry and are influenced by the  
73 ongoing climate change, due to rising concentrations of atmospheric CO<sub>2</sub> and  
74 other greenhouse gases. Ocean warming has increasing impacts on ocean  
75 ecosystems by modifying the ecophysiology and distribution of marine  
76 organisms, and by altering ocean circulation and stratification. Ocean ecosystems  
77 also are important components of the climate system, influencing the  
78 atmospheric abundance of radiative agents such as CO<sub>2</sub>, N<sub>2</sub>O, aerosols and the  
79 bio-optical properties of seawater and upper ocean physics (Bopp et al. 2013;  
80 Goldstein et al. 2003; Manizza et al. 2008; Schmittner and Galbraith 2008;  
81 Siegenthaler and Wenk 1984). Therefore, understanding the mechanisms  
82 controlling NPP and EP is essential for understanding the global cycles of carbon  
83 and other bioactive elements, and their links to climate. (Passow and Carlson  
84 2012).

Deleted: strongly

Deleted: warming conditions

85 Upper ocean stratification plays a key role in ocean biogeochemical processes.  
86 In particular, mixed layer depth (MLD) regulates the interplay between light  
87 availability for photosynthesis (Hannon et al. 2001) and nutrient supply to the,  
88 upper ocean (e.g., Pollard et al. 2009). Upper ocean stratification is defined here  
89 as the density difference between the surface and 200 m depth (Capotondi et al.  
90 2012), which is indicative of the degree of coupling and nutrient fluxes between  
91 the euphotic zone and the ocean interior. The density gradient at the base of the  
92 mixed layer affects entrainment processes, which play a crucial role in mixed  
93 layer deepening and in particle sinking/export from the euphotic zone.  
94 Stratification can also influence ocean ventilation (Luo et al. 2009), which has  
95 important consequences for oceanic uptake of carbon and oxygen. Thus, changes

Deleted: n many

Deleted: from the deep to

Deleted: s

101 in stratification over the remainder of the 21<sup>st</sup> century have the potential to  
102 influence NPP and EP across marine ecosystems.

103 Stratification tends to increase in response to ocean surface warming and  
104 freshening in 21st century climate change simulations. Increased stratification  
105 reduces the input of sub-surface nutrients to the euphotic zone and can lead to  
106 decreasing NPP and EP through increasing nutrient limitation. Many studies  
107 have suggested decreases in global NPP and EP over the 21 century using  
108 models with varying degrees of complexity (Bopp et al. 2001; Cabré et al. 2015;  
109 Dutkiewicz et al. 2013; Froelicher et al. 2009; Fung et al. 2005; Plattner et al. 2001;  
110 Schmittner et al. 2008). For the RCP8.5 scenario, CMIP5 ESM estimates of  
111 changes in export production range from -7 to -18% relative to 1990s and for  
112 NPP these changes range from -2 to -16% (Bopp et al. 2013).

113 The relative importance of different ecological controls on NPP and EP  
114 depends, in part, on an individual model's capacity to represent plankton  
115 functional types (PFT) (Jin et al. 2006; Le Quere et al. 2005) and their unique  
116 physiological and ecological characteristics, which determine how efficiently  
117 they are exported from surface waters. Increasing nutrient stress can shift  
118 phytoplankton community composition, favoring smaller phytoplankton, which  
119 are more efficient at nutrient uptake, over larger phytoplankton (Bopp et al. 2001;  
120 Steinacher et al. 2010; Vichi et al. 2011). These community shifts can modify the  
121 efficiency of carbon export to the interior ocean. However, the treatment of  
122 plankton communities is relatively simple in the CMIP5 models, with 1-3  
123 phytoplankton functional types and typically one zooplankton group (Bopp et al.  
124 2013).

125 Several previous studies have studied the biogeochemical response to  
126 climate change in the CMIP5 models. Bopp et al. (2013) examined output from 10

**Deleted:** . This typically occurs

**Moved (insertion) [1]**

**Deleted:** global warming simulations as atmospheric greenhouse gas concentrations continue to increase

**Deleted:** With sustained increases in warming, m

**Deleted:** document

**Deleted:** (Bopp et al. 2001; Cabré et al. 2015; Dutkiewicz et al. 2013; Froelicher et al. 2009; Fung et al. 2005; Plattner et al. 2001; Schmittner et al. 2008)

**Deleted:** whereas

**Deleted:** are smaller,

**Deleted:** varying

**Moved up [1]:** Increased stratification reduces the input of sub-surface nutrients to the euphotic zone and can lead to decreasing NPP and EP through increasing nutrient limitation.

**Deleted:** Increasing nutrient stress also can shift phytoplankton community composition, favoring smaller phytoplankton over larger phytoplankton (Bopp et al. 2001; Steinacher et al. 2010; Vichi et al. 2011).

**Deleted:** .

**Deleted:** For the CMIP5 biogeochemical models, the marine biological cycle is closed in the sense that nutrient uptake by phytoplankton, export of organic material into the thermocline, remineralization of organic material and transport of inorganic nutrients by the circulation are represented. In this regard, these models are suitable to study the response of NPP and EP to stratification changes.

**Deleted:** still

**Deleted:** most models carrying three or fewer classes

155 CMIP5 models emphasizing model mean biogeochemical responses to multiple  
156 stressors and trends over the 21<sup>st</sup> century relative to 1990s means for each model  
157 (also applying a correction for long-term trends in model output). Cabré et al.  
158 (2015) also analyzed the CMIP5 models examining changes between model  
159 output averaged over the period 1980-1999 with years 2080-2099. This study  
160 broke down the global output into different ocean biomes for analysis.  
161 Laufkötter et al. (2015a) also analyzed output from nine coupled climate-carbon  
162 ESMs including many of the CMIP5 models to study how climate change  
163 processes impact NPP comparing two twenty-year periods (2012-2031 and 2081-  
164 2100). They suggested strong roles for temperature and top-down grazing  
165 control in driving the NPP response, particularly at lower latitudes. Both Cabré  
166 et al. (2015) and Laufkötter et al. (2015) conclude that changing light levels were  
167 not a primary driver of changes in NPP except at the highest latitudes where  
168 there were strong changes in sea ice cover. Thus, we do not consider light effects  
169 in this work, where our focus is on the global-scale. More detailed regional  
170 studies of the CMIP5 model output have been carried out for the Arctic Ocean  
171 (Vancoppenolle et al., 2013) and the Southern Ocean (Leung et al., 2015; Hauck et  
172 al., 2015; and Ito et al., 2015).

173 We analyzed centennial-scale changes in NPP and EP in response to  
174 increasing surface stratification and other physical factors. We use historical  
175 (1850-2005) and Representative Concentration Pathway (RCP) 8.5 (2006-2100)  
176 ESM simulations from the fifth phase of the Coupled Model Inter-comparison  
177 Project (CMIP5). One goal of this study is to study long-term trends in NPP and  
178 EP under strong warming conditions to identify the mechanisms behind these  
179 changes, including the physical factors that regulate nutrient availability. We  
180 also examined variability in NPP, EP, and surface nutrient concentrations across

Formatted: Superscript

Deleted: Here w

Deleted: contributed to

Deleted: As a part of our analysis, w



184 the models, to highlight some of the large differences and uncertainties in the  
185 projections of climate change impacts on marine biogeochemistry.

186

## 187 **2 Methods**

188 We analyzed simulations from a set of 9 ESMs that contributed output to the  
189 Earth System Grid Federation as a part of CMIP5 (Taylor et al. 2012). Required  
190 physical ocean variables were temperature, salinity, and potential density;  
191 required biogeochemistry variables were macro-nutrients (nitrate, phosphate,  
192 and silicic acid), iron, chlorophyll, NPP and EP. The selection of the 9 models  
193 investigated here ([Table 1](#)) was based on the availability of these variables.

194 The historical and RCP8.5 simulations we analyzed had prescribed  
195 atmospheric CO<sub>2</sub> mole fractions and forcing from other greenhouse gases and  
196 aerosols, anthropogenic land use, and solar variability. Volcanic forcing also was  
197 included during the historical period. The RCP 8.5 is a strong warming scenario  
198 with an increase in radiative forcing of 8.5 W/m<sup>2</sup> by 2100 as atmospheric CO<sub>2</sub>  
199 mole fractions reach 936 ppm (Moss et al. 2010; van Vuuren et al. 2011). In the  
200 case where several ensemble members were available from an individual ESM,  
201 we analyzed only the first member.

202 A simple description of the 9 ESMs is presented in Tables 1 and 2.  
203 Atmospheric and ocean resolutions vary across the models (Table 1). Typical  
204 atmospheric horizontal grid resolution is ~2°, but it ranges from 0.94 to 3.8°.  
205 Typical ocean horizontal resolution is ~1°, ranging from 0.3° to 2°. In the vertical,  
206 there are 24 to 95 levels in the atmosphere and 31 to 63 levels in the ocean. All  
207 marine biogeochemical components are nutrient–phytoplankton–zooplankton–  
208 detritus (NPZD) models, but with varying degrees of complexity, illustrated for

**Deleted:** document how absolute concentrations and fluxes vary across the different models  
**Deleted:** considerable  
**Deleted:** y  
**Deleted:** CMIP5

**Deleted:** widely  
**Deleted:** different

216 instance by the number of phytoplankton functional groups (from 1 to 3) or  
217 limiting nutrients (from 3 to 5) that are explicitly represented (Table 2).

218 In our analysis, we used the CMIP5 variable denoting the vertical integration  
219 of NPP and sinking export of organic particles at 100 m (EP). We present global  
220 mean estimates as the area-weighted or volume-weighted mean by the grid-cell  
221 area/volume from an individual model. Monthly mean data are averaged to  
222 obtain annual means and the annual mean data are interpolated onto a common  
223  $1^{\circ}\times 1^{\circ}$  regular grid for the comparison of the 2-D fields.

224

### 225 **3 Results**

#### 226 **3.1 Stratification changes**

227 Stratification, defined here as the density difference between the depth of 200  
228 m and the surface, is a useful indicator of change in the upper ocean, as it  
229 integrates changes in both temperature and salinity. In Figure 1a, we present the  
230 time series of global mean stratification changes for the historical period and the  
231 RCP8.5 projection. All the models project an increase in stratification (ranging  
232 from 6% to 30% at 2100). However, the amplitude of stratification differs  
233 considerably across the models. The GFDL-ESM2M and MPI models are  
234 relatively close to the observed mean stratification in the WOA09 dataset (red  
235 square,  $1.81 \text{ kg/m}^3$ ) for the present era. NorESM1-ME shows the weakest  
236 stratification ( $1.74 \text{ kg/m}^3$ ) while the stratification in HadGEM2-ES is strongest  
237 ( $2.45 \text{ kg/m}^3$ ). Long-term trends are in general agreement across models, but the  
238 rate of stratification increase varies, with IPSL-CM5A-MR showing a more rapid  
239 increase while NorESM1-ME has the slowest increase in stratification.

240 Surface processes that decrease density can largely explain the stratification  
241 increase in the RCP8.5 projections. Global mean sea surface temperature (SST)

Deleted: s

Deleted:

244 warms by 2.6-3.5°C, accompanied by sea surface salinity (SSS) decreases of 0.05-  
245 0.25 psu over the 21<sup>st</sup> century (Figure 1). By 2100, the global mean SST ranges  
246 from 20.4°C (HadGEM2-ES) to 21.8°C (NorESM1-ME). Model spread decreases  
247 in the RCP8.5 projections in response to strong anthropogenic forcing (Figure 1b).  
248 The SSS shows a clear declining tendency from 1850 to 2100 (Figure 1).  
249 Compared to the WOA09 observational data, most of the models are too fresh at  
250 the surface in the 1990s, especially the HadGEM2-ES, which has the lowest global  
251 mean SSS. The model spread is partly due to internal variability simulated by the  
252 climate models. Model differences in spin up procedures, the way RCP scenarios  
253 are set up, and model climate sensitivities all likely contribute to the model  
254 spread (Knutti and Hegerl 2008; Szopa et al. 2013; Séférian et al., 2015).

Deleted: the

255 Vertical density profiles help to further explain the changes in stratification.  
256 Mean vertical profiles of density in the 1990s and the density change between the  
257 1990s and the 2090s show that all the models become more buoyant at the surface  
258 as a consequence of heating and/or freshening of the upper ocean (Figure S1).  
259 The density changes at the surface vary by almost a factor of two among models,  
260 from -1.1 kg/m<sup>3</sup> (HadGEM) to -0.6 kg/m<sup>3</sup> (GFDL-ES2M), but converge to a  
261 relatively narrow range (approximately -0.2 kg/m<sup>3</sup>) at 500 m depth. Most of the  
262 density change occurs between the surface and 200 m. Below 200 m, the density  
263 change in most of the models varies linearly with depth. Thus, our definition of  
264 the stratification index, as the density difference between the surface and 200 m,  
265 appears reasonable. The converging reductions in density among models at  
266 about 500 m agrees with some previous studies based on observations and  
267 CMIP3 models (Bindoff et al. 2007; Capotondi et al. 2012; Lyman et al. 2010).  
268 Compared to WOA09 data, the models generally underestimate the density of

Deleted: 2

Deleted: s

Deleted: s

Deleted: y

Deleted: data

275 the upper ocean (<150 m) and most models overestimate the density below 350 m  
276 (resulting in a positive stratification bias) (Figure S1a).

277 Vertical profiles of temperature and salinity from each model are also shown  
278 in Figure S1. The surface ocean exhibits strong warming of 1.7-3.5°C by the 2090s  
279 and the warming magnitude declines quickly with depth, which is associated  
280 with the heat uptake capacity of individual models. For instance, GFDL models  
281 seem to be more efficient in transporting heat downward than the IPSL models.  
282 Above 300 m, the temperature changes vary widely among the models.

283 Temperature changes as a function of depth are complex, and model-to-model  
284 differences may be related to a number of factors including rates of vertical  
285 mixing and the seasonal thermocline dynamics. At the depth of 500 m, the mean  
286 temperature change converges at about 1.2°C. The ocean heat uptake capacity is

287 linked to ocean diapycnal mixing, and other processes, such as mixing by  
288 mesoscale eddies, which influence the rates of warming in the ocean interior. It is

289 assumed that a model with a weak vertical temperature gradient in the control  
290 state has a larger capacity for downward heat transport (Kuhlbrodt and Gregory  
291 2012). The heat uptake capacity of GFDL models could be large as the  
292 temperature gradients are weaker than for other models. The large model spread  
293 in temperature profiles suggests considerable differences and uncertainties in the  
294 parameterizations of these physical processes across the models. Vertical profiles

295 of salinity are more scattered than for temperature (Figure S1c). In the 1990s,  
296 most of the models underestimate salinity from the surface down to 550 m.

297 Surface salinity is generally biased low by 0.05-0.25 psu. Most of the freshening  
298 with climate change takes place above 100 m, which also acts to increase  
299 stratification. Note that the salinity increases at 100-300m in some models (IPSL,

Deleted: C

Deleted: is important because it

Deleted: ,

Deleted: major

Deleted: helps

305 GFDL-ESM2M, HadGEM2-ES) partially compensates the impact of rising  
306 temperatures on density.

307 The relative contribution (%) of temperature change to the stratification  
308 change from the 1990s to the 2090s is shown in Figure S2. Previous studies have  
309 shown that salinity contributes significantly to the stratification changes at high  
310 latitudes (>40°) in both hemispheres and in the North Pacific as a consequence of  
311 increases in precipitation (e.g., Bindoff et al. 2007). From our comparisons,  
312 temperature dominates the stratification changes in the tropical and sub-tropical  
313 regions (Figure S2). Salinity dominates the stratification changes in the much of  
314 the Arctic Ocean and in the high-latitude North Atlantic. [While stratification is a  
315 function of SSS and SST to a good approximation](#) (Cabr e et al. 2015), [stratification  
316 change at high latitudes is also dependent on temperature and salinity at depth  
317 as vertical mixing and exchange are stronger](#).

Deleted: 3

Deleted: is stronger than the Tropical ocean.

318 In some regions the spatial distributions and the driving process differs  
319 substantially across models. Generally, the models agree well in the tropics and  
320 subtropical gyres [that surface warming drives](#) increasing stratification. In the  
321 high latitude North Atlantic, the subpolar Pacific and the western Pacific Ocean,  
322 there is [weaker](#) agreement across the models. In the subtropical gyre of the south  
323 Pacific, stratification changes in the IPSL and CESM1-BGC models are more  
324 dominated by temperature changes, while the other models exhibit more  
325 complicated spatial patterns. In the North Atlantic, salinity contributes more in  
326 the IPSL and HadGEM2 models than in other models. The southeastern Pacific is  
327 more dominated by salinity in the two GFDL models. In the Southern Ocean, the  
328 models show relatively large contributions from both salinity and temperature  
329 but with complicated spatial patterns that differ substantially across models.  
330 Projections for the regions where the models do not agree even on the driving

333 factor should be viewed with more caution. [Climate change trends in these](#)  
334 [regions tend to be projected with less significance across models, for instance,](#)  
335 [shown in Fig. 1 of Cabré et al. \(2015\).](#)

Deleted: s

336 The spatial patterns of the changes in stratification are displayed for all the  
337 models in Figure 2. [Stratification increases globally in all the models with climate](#)  
338 [change.](#) Nearly all the models predict large increases in stratification in the  
339 western tropical Pacific, the tropical Indian Ocean, the Arctic Ocean, and in the  
340 high latitude North Atlantic (particularly in the Labrador Sea). [The Southern](#)  
341 [Ocean has weaker increases in stratification, partly because the surface layer](#)  
342 [mixing and upwelling are intensified due to the poleward shift of strengthened](#)  
343 [westerly jets](#) (Swart and Fyfe 2012; [Sallée et al., 2013](#); [Bracegirdle et al., 2013](#);  
344 [Hauck et al., 2015](#); [Leung et al., 2015](#); [Ito et al., 2015](#)). Our stratification index may  
345 underestimate the changes in the high latitude North Atlantic, as the relatively  
346 deep mixing means that temperature and salinity at 200m depth are changing  
347 much more rapidly than in other regions. Reductions in the deep winter mixing  
348 and NADW formation in this region are a common pattern seen in strong  
349 warming climate simulations (e.g., [Cheng et al., 2013](#); [Schwinger et al., 2014](#)).  
350 Less drastic increases in stratification are seen over much of the rest of the oceans,  
351 with only a few small regions showing decreases in stratification [in some models](#).  
352 [An](#) exception is the HadGEM2-ES model which has large stratification  
353 reductions in the Arctic (Figure 2).

Deleted: shows less

Deleted: in this region

Deleted: 4

### 354 **3.2 Surface Nutrient Trends with Climate Change**

355 One of the key factors determining global NPP is nutrient availability in the  
356 euphotic zone. Time series of global mean nutrient (0-100m) concentrations for  
357 nitrate (NO<sub>3</sub>), phosphate (PO<sub>4</sub>), silicic acid (SiO<sub>4</sub>) and dissolved iron (dFe) are  
358 presented in Figure 3. The magnitude of surface nutrient concentrations differs

Deleted: 5

364 substantially across the models (varying by a factor of ~1.5-2, and by a factor of 5  
365 for dissolved iron). The IPSL models have relatively low surface nutrient  
366 concentrations. Compared to the WOA09, 2 models overestimate phosphate  
367 (CESM1(BGC) and GFDL-ESM2G) and 5 models overestimate nitrate. All of the  
368 models overestimate the silicic acid observations, with the exception of  
369 CESM1(BGC). The CESM1(BGC) model overestimates surface phosphate  
370 concentrations initially, due to excessive nitrogen limitation, but then shows the  
371 strongest surface phosphate declines over the 21<sup>st</sup> century (Figure 3; Moore et al.  
372 2013).

Deleted: 4

373 Over the entire period from 1850-2100, the models all display decreasing  
374 trends for surface nitrate, phosphate and silicic acid. Interestingly, surface iron  
375 concentrations increase modestly in all but one of the models by 4-10%. Changes  
376 in iron concentrations impact marine productivity, nitrogen fixation rates, and  
377 oceanic net CO<sub>2</sub> uptake. In the CMIP5 simulations, iron inputs to the oceans were  
378 held constant over time, so the increasing surface iron concentrations may reflect  
379 increasing macronutrient limitation of phytoplankton growth, leading to reduced  
380 biological uptake of iron. The reductions in the sinking export flux also reduce  
381 the particle scavenging loss term for dissolved iron. In the CESM1-BGC model,  
382 increased production in the High Nutrient, Low Chlorophyll (HNLC) regions  
383 offset ~25% of the reduction observed in the macronutrient-limited areas with  
384 climate change, while changing circulation patterns also altered the lateral  
385 transport of iron within the oceans (Misumi et al. 2014; Moore et al. 2013).

Deleted: .

Deleted: This can be partly attributed to enhanced stratification, which traps and concentrates more iron in the surface (Steinacher et al. 2010).

Deleted: may

386 The relative changes in nutrient concentrations (0-100m) (normalized to  
387 1990s means) are presented in Figure 4. The relative changes in the historical run  
388 show a consistent pattern across the models for nitrate, phosphate and dissolved  
389 iron (except for HadGEM2-ES). In the RCP8.5 projection, the models show

396 diverging estimates of magnitude of the relative changes. For nitrate, the  
397 reductions range between -3 to -14% and the phosphate changes range between -  
398 3 to -20%. Silicic acid and iron trends are even more variable than for nitrate and  
399 phosphate. For silicic acid, there are 3 models showing slight increases, while the  
400 others exhibit decreases ranging from ~5-17%. The variability in relative change  
401 in silicic acid concentration in the RCP8.5 is likely associated with changes in  
402 plankton community and variable diatom production (Bopp et al. 2005). All of  
403 the models include some representation of diatoms (Table 2) but the match to  
404 observed silicic acid for the current era is generally poor (Figure 3).

405 The spatial distributions of mean nitrate concentration for 0-100 m in the  
406 1990s are shown in Figure S3. The CMIP5 models reproduce key observed  
407 features of the basin scale distributions of surface nitrate. For example, in the  
408 eastern equatorial Pacific, Southern Ocean, subarctic North Atlantic and  
409 subarctic Pacific exhibit elevated nitrate concentrations in all the models. In the  
410 subtropical gyres of the Atlantic and Pacific basins, the mean nitrate  
411 concentration is low. However, inter-model comparisons show clear  
412 disagreements in some key regions. For example, the details of the high-nitrate  
413 water distributions vary considerably in the eastern equatorial Pacific. The  
414 HNLC condition extends too far north and south of the equator in some models,  
415 and too far to the west in others (Figure S3). The models also differ in the  
416 intensity and extent of high nitrate concentration waters in the subarctic North  
417 Pacific, where 6 of 9 models show lower nitrate concentrations than the WOA09  
418 data (MPI-ESM-LR, MPI-ESM-MR and HadGEM2-ES are closest to observations).  
419 There are also differences in the Arabian Sea and Bay of Bengal, where most  
420 models underestimate nitrate concentrations except the GFDL-ESM2M and MPI-  
421 ESM-LR models.

**Deleted:** The larger uncertainties in the projections of silicic acid concentrations emphasize the need to improve model representations of phytoplankton community structure in marine ecosystem models (Dutkiewicz et al. 2013). With respect to dissolved iron, the 8 models present an increase of 4-10% relative to 1990s, while in the NorESM-ME model surface iron is reduced by 3%. Pre-industrial levels of iron and silicic acid appear too low for the HadGEM2-ES model (Figure 6).

**Deleted:** the

**Deleted:** (

**Deleted:** 7)

**Deleted:** 7

**Deleted:** r

**Deleted:** clear



436 Inter-model spread in NPP during the 1990s is pronounced, with NPP as low  
437 as 29 PgC yr<sup>-1</sup> (IPSL-CM5A-LR and IPSL-CM5A-MR), while NPP in one model  
438 exceeds 75 PgC yr<sup>-1</sup> (GFDL-ESM2M) (Table 3, Figure 5). [In addition, the spatial](#)  
439 [pattern of NPP is not well represented by the multi-model mean](#) (Bopp et al.  
440 2013). Satellite based estimation of NPP is approximately 50 PgC yr<sup>-1</sup> (Behrenfeld  
441 et al. 2006; Carr et al. 2006; [Anav et al., 2013](#)). The MPI-ES-MR and CESM1-BGC  
442 models had NPP of 49.8 PgC yr<sup>-1</sup> and 54.2 PgC yr<sup>-1</sup>, closer to the satellite-based  
443 estimates, [and the observationally constrained model estimate of 56 PgC yr<sup>-1</sup> by](#)  
444 [Buitenhuis et al. \(2013a\)](#). The magnitude of EP also [varies](#) substantially across  
445 models in the 1990s, ranging from 4.4 to 7.2 PgC yr<sup>-1</sup> (Table 3).

Deleted: .  
Deleted: differs  
Deleted: PgC yr<sup>-1</sup>

### 446 3.3 Climate Change Impacts on NPP and EP

447 All of the models exhibit decreasing trends in [global NPP](#) and EP with  
448 climate change [as shown in previous studies](#) (Bopp et al. 2013; [Cabré et al., 2015;](#)  
449 [Laufkötter et al., 2015](#)), and most models show more rapid decreases during [the](#)  
450 middle to latter part of the 21<sup>st</sup> century (Figures 5-6, Table 3). All nine models  
451 project decreases in export production under RCP8.5 exceeding 5% relative to  
452 levels in the 1990s, whereas the response for NPP is divided into 2 groups after  
453 2020. The CESM1(BGC) and GDFL models experience smaller changes in NPP (<  
454 5% relative to 1990s) while other models have larger decreases (8-16%). The  
455 largest relative change for NPP is about -16% (MPI-ESM-LR). The EP decreases  
456 range from 7% (GFDL-ESM2G) to 28% (IPSL-CM5A-LR). [Cabré et al. \(2015\)](#)  
457 [showed reductions in NPP and EP for all biomes, except at the highest latitudes.](#)  
458 The reductions in global NPP and EP co-vary with [the](#) increases in stratification  
459 (Figure 6). [By](#) the 2090s, stratification increases by about 16% in GFDL-ESM2M  
460 and up to 33% in HadGEM1-ES. The rate of stratification increase is slower in the

Deleted:  
Deleted: Dutkiewicz et al. 2013  
Deleted: 8-9

467 two GFDL models and CESM1(BGC), which also agrees with the slower rates of  
468 relative NPP and EP change.

469 The variability across models in NPP is substantially larger than that seen in  
470 EP (Table 3). The normalized standard deviation was +/- 27 % for NPP, but only  
471 +/- 12 % for EP in the 1990s. [The large spread in simulated NPP and its response](#)  
472 [to climate change was also noted by Laufkötter et al. \(2015a\)](#). Seven of the nine  
473 models have an EP between 6 and 7.2 PgC yr<sup>-1</sup> in the 1990s, [and](#) the HadGEM2-  
474 ES and GFDL-ESM2G models had lower EP (< 5 PgC yr<sup>-1</sup>). EP is tightly coupled  
475 to new nutrient inputs to the euphotic zone in these models. NPP is less tightly  
476 coupled as the fraction of regenerated production varies across the models, and  
477 can vary spatially and temporally within [some](#) models. Thus, the large spread in  
478 NPP is not mainly a function of the different physical models and their transport  
479 of nutrients to the euphotic zone, but rather it is strongly impacted by the  
480 [community structure and](#) export efficiency inherent in the models, and the  
481 resulting varying levels of regenerated production.

482 The sinking [carbon](#) flux out of the euphotic zone to net primary production  
483 ratio ([particle export ratio or pe-ratio](#)) is a measure of the export efficiency and  
484 also reflects the variable contribution of regenerated production to total NPP  
485 (Dugdale and Goering 1967; [Eppley and Peterson, 1979](#); Dunne et al., 2007). High  
486 pe-ratio values are typically associated with productive ecosystems dominated  
487 by larger phytoplankton (often diatoms, [Buesseler, 1998](#); [Boyd and Newton,](#)  
488 [1989](#)), while low pe-ratios are associated with oligotrophic food webs with most  
489 carbon flow through the microbial loop ([Pomeroy, 1974](#); Azam et al. 1983). The  
490 CMIP5 models that include both large and small phytoplankton, assume [a](#) higher  
491 export efficiency for the large phytoplankton ([Moore et al., 2004; 2013](#); Aumont  
492 and Bopp 2006; [Séférian et al. 2013](#); Tjiputra et al. 2013; [Laufkötter et al., 2015b](#)).

Formatted: Font color: Dark Red

Deleted: ; Eppley and Peterson 1979

494 The fraction of grazed material routed to sinking export is higher, often by a  
495 factor of 3-6 than the fraction routed to sinking export for the small  
496 phytoplankton (see Laufkötter et al., 2015b for detailed discussion). Diatoms are  
497 also likely to dominate phytoplankton blooms in these models. This can drive  
498 additional, very efficient, export through aggregation, further enhancing the  
499 differences in export efficiency between large and small phytoplankton. Relative  
500 to the 1990s, six of the nine models show decreasing trends in the pe-ratio (up to  
501 10% reduction) (Figures 5-6, Table 3; see also Cabré et al., 2015). Diatoms  
502 accounted for a smaller percentage of NPP in the 2090s than in the 1990s in all  
503 the models, except for the MPI model, where nearly all of the production is by  
504 diatoms and the smallest phytoplankton are not explicitly represented (Table 3).

Deleted: s

Deleted: 8 and 9

Deleted: the

Deleted: included

Deleted: The declines in pe-ratio and in the percent of NPP by diatoms were modest at the global scale, but larger shifts were seen in some regions (see following sections).

Deleted: Relative changes in global NPP between the 1990s and the 2090s are plotted against relative change in stratification in Figure 10a.

Deleted: In this paper, w

Deleted:

Deleted: s

Deleted: the 1990s and 2090s

Deleted: , which is different from the results in

Deleted: (

Deleted: )

Deleted: and

Deleted: (

### 505 3.4 Increasing Stratification and Declining Nutrients, NPP, and EP

506 We quantify the relations between stratification and key biogeochemical  
507 variables with annual model output over the entire time period of 1850-2100.

508 This approach is more robust than focusing only on the differences between  
509 beginning and end of century output (Bopp et al., 2013; Cabré et al., 2015;  
510 Laufkötter et al., 2015). Relative changes in global NPP between the 1990s and  
511 the 2090s are plotted against the relative change in stratification in Figure 7a.

512 Across all the ESMs, a good relationship is found with a correlation  $r^2=0.72$ .  
513 Larger relative increases in stratification correspond to larger declines in NPP. In  
514 addition, the globally-fitted line with a slope of 0.38 separates the models into  
515 two groups. In one group (GFDL, IPSL and CESM1-BGC), the NPP reductions  
516 are more modest as stratification increases; the other group is composed of the  
517 two MPI models, HadGEM1-ES and the NorESM model, which show more  
518 intense and linear reductions in NPP with increasing stratification. The reduction  
519 of NPP can be partly explained by nutrient changes responding to stratification

Deleted: is

Deleted: a

Deleted: rapid,

Deleted: fairly

543 increases. Across the models, surface nitrate and phosphate concentrations  
544 clearly decline as the stratification is enhanced (Figure 7c and 7d, with  $r^2$  of 0.80  
545 and 0.82, respectively). Note that all of these trends are robust across the full time  
546 series. Compared to the 1990s, the preindustrial stratification is weaker, surface  
547 nutrient concentrations are higher, and NPP and EP are elevated (Figures 3-7).  
548 The response of surface silicic acid to increasing stratification is more variable,  
549 The projected changes are more divided, as three models (MPI-ESM-LR, MPI-  
550 ESM-MR and HadGEM1-ES) show slight increases and the others show  
551 reductions in surface silicic acid concentrations (Figure 7b).

Deleted: 10

Deleted: 10

Deleted: much

Deleted:

Deleted: 10

552 EP is even more closely related to the stratification changes ( $R^2=0.89$ ) than  
553 NPP (Figure 7e). The EP change is also closely related to the NPP changes. EP  
554 decreases by up to 20% (Figure 7e) whereas NPP decreases by 10-18%. The  
555 models display two patterns in terms of the response of NPP and EP to climate  
556 change. The first group includes five models (IPSL models, CESM1(BGC) and the  
557 GFDL models) where the relative declines in NPP are smaller than the relative  
558 declines in EP by a factor of 2 or more (Figure 6 and Table 3). In this group, the  
559 EP drops by about 10% and the NPP decreases by 5% or less. In the remaining  
560 models the relative declines in EP and NPP are larger and more similar in  
561 magnitude. For example, both EP and NPP decrease by about 14% in the  
562 HadGEM2-ES model. The differential declines in NPP and EP in the first group  
563 of models documents declining export efficiency for the ocean biological pump,  
564 driven by phytoplankton community shifts and a decreased contribution to NPP  
565 by large phytoplankton (diatoms) (see below and Figures 6-10; also Cabré et al.,  
566 2015).

Deleted: 10

Deleted: 10

Deleted: 9

Deleted: and

Deleted: 9-13

567 Reduced nutrient availability seems to be a major contributor to declines in  
568 NPP and EP. However, the relationship varies from one model to another

579 because growth and export are complicated functions of macronutrient  
580 limitation, temperature, irradiance and iron limitation, as well as the routing of  
581 organic matter within the ecosystem that drives export efficiency. Higher  
582 metabolic rates with warming can be compensated to a large degree by changes  
583 in the supply of nutrients and altered light in terms of globally integrated  
584 productivity (Dutkiewicz et al. 2013). The NPP response is also strongly  
585 impacted by phytoplankton community structure, which modifies export  
586 efficiency, and the corresponding magnitude of the regenerated primary  
587 production. For the IPSL, CESM1(BGC), and GFDL models that show larger  
588 declines in EP than in NPP, this pattern is driven by a decreasing contribution to  
589 total NPP by large phytoplankton (Table 3, Figures 8-9). Most of the primary  
590 production in these models is by smaller phytoplankton. The GFDL models  
591 express this pattern most strongly, with minimal declines in NPP, despite  
592 declines in EP approaching 10% (Figure 6, and Table 3). The other models tend to  
593 have production that is dominated by diatoms, and do not capture the  
594 community shifts towards increasing small phytoplankton dominance (and  
595 reduced export efficiency) under increasing nutrient stress. The declines in NPP  
596 with increasing stratification are more linear and more similar in magnitude to  
597 the declines in EP (Figure 7, panels a, b, and h). Thus, there are also very strong  
598 correlations between the climate-driven changes in the fractional contribution of  
599 diatoms to NPP and both the changes in stratification and the changes in EP  
600 (Figure 7, panels f and g, correlations of  $r^2=0.85$  and  $r^2=0.95$ , both much higher  
601 than the correlation between changing stratification and NPP,  $r^2=0.71$ ). Cabré et  
602 al. (2015) found similar patterns relating community composition, NPP, and EP  
603 comparing the period from 1980-1999 with 2080-2099, across low to mid-latitude  
604 biomes.

Deleted: controls the

Deleted: is

Deleted: on

Deleted: 11 and 12

Deleted: 9

Deleted: 10

Deleted: 10

Deleted: 11

Deleted: world

Deleted: will

Deleted: XXXX

Deleted: 12

612 Some of these patterns are illustrated in Figure 8, which shows the  
613 contribution of diatoms (large phytoplankton) to NPP for the 1990s. Most of the  
614 models show elevated diatom production at high latitudes and lower diatom  
615 contributions in the subtropical gyres. However, there are large discrepancies in  
616 the magnitude of the diatom contribution, ranging from about 30% to more than  
617 90% in the Arctic Ocean, for example. At the global-scale diatoms account for  
618 only 9.4% of NPP in the GFDL-ESM2M model and reach a maximum of 91% in  
619 the MPI-ESM-MR model (Table 3). The large variability across the models  
620 reflects, in part, the lack of an observational dataset to constrain phytoplankton  
621 community composition, at the time these models were being developed. The  
622 new globally-gridded ocean atlas of plankton functional types, MAREDAT  
623 (Buitenhuis et al. 2013) has started to fill this gap, and should lead to improved  
624 representations of plankton community structure in the future as the dataset  
625 becomes increasingly populated and is entrained into model development and  
626 validation. [Remote sensing estimates of phytoplankton community composition  
627 and size class structures are also providing useful constraints for global-scale  
628 modeling efforts \(e.g., Alvain et al., 2005; Hirata et al., 2008; Kostadinov et al.,  
629 2009; Siegel et al., 2014\).](#)

630 The spatial patterns of the shifts in phytoplankton community composition  
631 with climate change are illustrated in Figure 9, where we plot the change in the  
632 percentage of NPP by diatoms (2090s – 1990s). There are some robust trends  
633 across the models. One of the areas with the biggest declines in diatom  
634 production is the high-latitude North Atlantic. This region typically has some of  
635 the biggest stratification increases with climate change, greatly reducing the deep  
636 winter mixing that entrains nutrients to the surface (Moore et al. 2013; [Cheng et  
637 al., 2013](#); Randerson et al. 2015). Nearly all the models also show large declines in

643 diatom contributions to production in the Arctic Ocean. The CMIP5 models  
644 show consistent trends of increasing stratification, declining surface nutrient  
645 concentrations, and a longer growing season with climate change in the Arctic  
646 (Vancoppenolle et al. 2013). Increasing surface temperatures and dramatic  
647 declines in the sea ice cover allow for a longer growing season with climate  
648 change. Thus, nutrients in surface waters are more completely used up by  
649 summer's end, leading to community shifts with decreased diatom production  
650 and an increased fraction of production by smaller phytoplankton. In the CESM-  
651 BGC model, this community shift allows for a small increase in central Arctic  
652 NPP, even as export production and surface nutrient concentrations decline, due  
653 to the increased fraction of NPP by small phytoplankton and the resulting  
654 increases in regenerated production (Moore et al., 2013).

655 All of the models show some increase in the fraction of NPP by diatoms in  
656 the Southern Ocean (Figure 9). The increase is particularly strong in the CESM1-  
657 BGC, IPSL, and GFDL models. Most of the models also show some increased  
658 diatom production in the tropical Pacific. Bopp et al. (2005) also found decreasing  
659 diatom production in the Arctic and high-latitude North Atlantic, with some  
660 increases in the Southern Ocean under a strong warming climate scenario.  
661 Steinacher et al. (2010) also found declining productivity in the North Atlantic,  
662 and shifts in the export ratio due to phytoplankton community shifts with  
663 decreasing diatom production. The earlier version of the CESM used in that  
664 study (CCSM3) showed only small shifts in export ratios with climate change, as  
665 the range in export ratios and the differences in export efficiencies between large  
666 and small phytoplankton were smaller than in the CESM (Moore et al. 2013;  
667 Steinacher et al. 2010). Three models in this study (HadGEM2-ES and the MPI  
668 models) show increased diatom production in the low latitudes (Figure 9).

Deleted: 12

Deleted: Bopp et al. (2005)

Deleted: r

Deleted: (

Deleted: Steinacher et al. (2010)

Deleted: (Steinacher et al., 2010; Moore et al., 2013)

Deleted: across

Deleted: 12

677 However, the diatoms dominate production nearly everywhere in these three  
678 models (Figure 8).

679 There are also large inter-model differences in the spatial patterns of the pe-  
680 ratio (Figure 10). Some of the models (GFDL, IPSL, CESM-BGC) show a close  
681 correlation between the pe-ratio and diatom production (compare Figures 8 and  
682 10), due to the enhanced export efficiency for diatoms (large phytoplankton)  
683 built into the models. Thus, there is a very high correlation between the changing  
684 contribution of diatoms to NPP and the changes in EP (Figure 7, panel g, Table 3).

685 The MPI model includes one phytoplankton group and has an essentially  
686 constant pe-ratio of 0.15, explaining the linearity of the changes in NPP and EP  
687 with warming (Figures 8 and 10). Production in the HadGEM1-ES model is  
688 dominated nearly everywhere by the diatoms (Figure 8). Therefore, the MPI and  
689 HadGEM models cannot capture a shift towards increasing small phytoplankton  
690 dominance under declining surface nutrient concentrations. This leads to export  
691 production being closely correlated with diatom production in these models as  
692 most production is by diatoms, as well as in the other models where diatoms are  
693 assumed to export more efficiently but account for a smaller fraction of total NPP  
694 (Table 3).

695 There is also a strong correlation between the declines in the fraction of NPP  
696 by diatoms and declines in the pe-ratio (compare Figures 7, 9 and 11). The largest  
697 declines in the pe-ratio are seen in the Arctic and the high-latitude North Atlantic,  
698 regions where diatom production also decreased. The GFDL, IPSL, and  
699 CESM1(BGC) models also show some reductions in pe-ratio in the subarctic  
700 North Pacific, but the spatial patterns are inconsistent (Figure 11). The models  
701 display considerable variability in the degree of stratification increase and in the

Deleted: T

Deleted: 11

Deleted: 3

Deleted: Most

Deleted: 11

Deleted: 3

Deleted: 10

Deleted: 11

Deleted: 3

Deleted: 11

Deleted: 12

Deleted: 14

Deleted: 4



715 dominant factor driving these changes in the subarctic North Pacific (Figures S2  
716 and 2).

717 The correlation for the relationship between the changing percentage of NPP  
718 by diatoms versus the changes in EP across all the models has an  $r^2$  value of 0.96  
719 and a slope with a value close to 1 (0.94, Figure 7g) indicating that phytoplankton  
720 community structure plays a dominant role in determining the responses of NPP,  
721 EP, and the pe-ratio to climate change. The biggest declines in the fraction of  
722 production by diatoms and pe-ratios are in precisely the areas where some of the  
723 largest increases in upper ocean stratification are seen, along with declining  
724 surface nutrient concentrations, as in the Arctic Ocean and in the high latitude  
725 North Atlantic (Figures 6-8; see also Moore et al., 2013; Steinacher et al., 2010;  
726 Cabré et al., 2015).

### 727 **3.5 Projected Changes in NPP, EP and Stratification Biases**

728 At global scale, the CMIP5 models show considerable stratification biases for  
729 the 1990s when compared to the WOA09 data (Figure 1, Table 3). Only the  
730 GFDL-ESM2M model is within 10% of the observed value. From the density  
731 profiles as well (Figure S1), it is apparent that most of the models have stronger  
732 stratification in the 1990s than seen in the observations. Liu et al. (2014) argued  
733 that climate bias is important when projecting the impact of climate change on  
734 land surface processes and Hoffman et al. (2014) documented this for  
735 atmospheric CO<sub>2</sub> mole fractions. Here, we examine how stratification biases in  
736 the 1990s may affect model projections of NPP and EP in the 2090s.

737 Models with stronger bias in the 1990s for surface stratification tend to  
738 predict larger climate-induced declines in both NPP and EP (Figure 12,  $r^2=0.47$   
739 and  $r^2=0.54$ , respectively). The slopes are plotted when the correlation is  
740 significant at >95% level. Five of the models have positive biases in stratification

Deleted: 3

Deleted: 4

Deleted: 10

Deleted: 9-11

Deleted: (

Deleted: )

Deleted: (

Deleted: )

Deleted: 2

Deleted: (Figures 2 and 15)

Deleted: ,

Deleted: 5

Deleted: 4

754 for the current era that exceed 20%. These models also show the largest relative  
755 increases in stratification with climate change of 26-30% (Figure 12, Table 3). The  
756 remaining four models (GFDL models, CESM1-BGC, and NorESM1-ME) do a  
757 better job of simulating observed stratification for the current era, and predict  
758 relative increases in stratification over the 21<sup>st</sup> century that are roughly half as  
759 large, ranging from ~15-18%. This suggests that the more biased models (for the  
760 1990s) may be overestimating the projected reductions in NPP and EP for the end  
761 of the century.

Deleted: 5

Deleted: 4

Deleted:

Deleted: edicted

762

#### 763 **4 Discussion and Conclusions**

764 The ESMs analyzed here have different resolutions and incorporate marine  
765 biogeochemical-ecosystem models with different mechanisms and degrees of  
766 complexity. We find this set of models has consistent trends of increasing  
767 stratification and decreasing NPP and EP. However, a large model spread is  
768 apparent for the 1990s, particularly for NPP, and in the relative changes to NPP  
769 and EP over the 21<sup>st</sup> century due to climate change. NPP is reduced by 2-18% in  
770 the 2090s and EP is reduced by 7-20%. Mean stratification increased by 16%  
771 (GFDL-ESM2M) to 33% (HadGEM1-ES) from the 1990s to the 2090s. Under  
772 strong warming scenarios like RCP8.5, ocean stratification will continue to  
773 rapidly increase after the year 2100 in all of these models (Randerson et al., 2015).

Deleted: by

Deleted: increasing

774 The strongly linear relationship between stratification increases and EP  
775 decreases seen within each model and across all the models (Figures 7 and 12)  
776 indicates a strong bottom up control on EP, through declining upward nutrient  
777 flux to the euphotic zone. Declining surface nutrient concentrations are seen in  
778 all the models with climate change under the RCP 8.5 scenario (Figures 5-6).  
779 Nitrate is reduced by 3 to 14% and phosphate is reduced by 3 to 20%. Changes in

Deleted: 10

Deleted: 5

Deleted: es

Deleted: and

790 surface silicic acid and iron concentrations are more variable across the models.  
791 For silicic acid, there are 3 models showing slight increases, while the others  
792 exhibit decreases of 5-17%. With respect to iron, 8 models indicate an increase of  
793 4-10% relative to the 1990s; with the exception being the NorESM-ME model,  
794 which is reduced by 3%. Changes in the temperature and light fields also have  
795 impacts on EP in some regions, but increasing stratification and nutrient stress,  
796 and the resulting impacts on phytoplankton community composition and EP is  
797 the dominate process at the global scale. On a global scale, over the full 1850-2100  
798 time period, the changes in NPP and EP are more highly correlated with the  
799 changes in stratification, than with the changes in SST ( $r^2$  0.72 for stratification-  
800 NPP and 0.66 for SST-NPP, Figure 7). This is because that the stratification metric  
801 captures both the temperature-driven changes that dominate at low to mid-  
802 latitudes, and the salinity-driven changes at higher latitudes. The relationship  
803 between the change of light levels and NPP was shown to be significant only in  
804 the sea-ice covered area of south hemisphere by Cabré et al. (2015). The  
805 temperature-driven increases in growth rates are offset by reduced nutrient  
806 supply in many regions as stratification is increased (Bopp et al. 2005; Cabré et al.  
807 2015).

Formatted: Superscript

Deleted: PAR

Deleted: of

Deleted: is also

Deleted: outcompeted

Deleted: and PP

Comment [WF1]: This paragraph is to address the 1st specific comment of reviewer #1.

Deleted: 10

Deleted: ,

Deleted: s in NPP

808 Simulated NPP and its response to climate change are both more variable  
809 across the models than EP, and are less strongly correlated with changes in  
810 stratification (Figure 7). This is driven by model differences in the export  
811 efficiency of the biological pump and its relation to phytoplankton community  
812 structure. The models that allow for shifts in phytoplankton community  
813 structure, whereby increasing nutrient stress gives competitive advantage to  
814 smaller cells over larger cells, show strongly non-linear NPP response to climate  
815 change. NPP declines less rapidly than EP with increasing nutrient stress, as the

824 percentage of NPP by large cells declines and export efficiency decreases (and  
825 the regenerated production fraction increases). Models without this dynamic  
826 community composition and export efficiency show a much more linear NPP  
827 response to climate change (Figure 7). Thus, projections of the response of NPP  
828 to climate change in the CMIP5 models are critically dependent on the simulated  
829 phytoplankton community structure, the efficiency of the biological pump, and  
830 the resulting (highly variable) levels of regenerated production.

831 Spatial patterns of diatom productivity are influenced by changes in surface  
832 nutrients and the resulting shifts in plankton community composition. The  
833 response of the %NPP by diatoms depends on several factors, including whether  
834 they were a small or large component of the community initially. Therefore, the  
835 spatial patterns of changes in stratification and %NPP by diatoms can differ  
836 (Figure 2, and Figure 9). In the paper, the largest decreases are seen in areas with  
837 high diatom production initially and large increases in stratification, particularly  
838 in the Northern Hemisphere, leading to North-South hemispheric asymmetry  
839 (Marinov et al., 2013; Cabré et al., 2015). In the Southern Ocean, the winds that  
840 drive upwelling, strengthen and shift poleward with climate change, influencing  
841 iron supply and productivity patterns (Sallée et al., 2013; Leung et al., 2015).

842 The large spread in the simulated NPP rates for the 1990s and the variability  
843 seen across models in the response of NPP to climate change introduce  
844 challenges for climate impact and risk assessment, as NPP is a key product of  
845 both terrestrial and marine ecosystem models, and changes to NPP are perhaps  
846 the most cited result from this class of models. We have demonstrated that the  
847 wide spread seen in simulated NPP is not due to the different physical  
848 circulation models and the flux of nutrients they deliver to surface waters, but  
849 rather to the efficiency of the biological pump (tied to community structure in

Deleted: the percentage of

Deleted: less

Deleted: 10

Deleted: , nutrient stress in the high latitudes,

Deleted: may be different

Deleted: 4

Deleted: 12

Deleted: in these models

Deleted: The wind-driven, poleward shift in the Southern Ocean subpolar-subtropical boundary results in a poleward shift and increase in the frontal diatom bloom (Marinov et al. 2013). Biogeochemical response to climate change may also depend on the inter-hemispheric asymmetry (Cabré et al. 2015).

863 most models) and the resulting levels of regenerated primary production (see  
864 also Cabré et al., 2015). Changes in EP are an additional useful metric of climate  
865 impacts on marine ecosystems. EP is more strongly tied to climate feedback, as it  
866 is mainly the fixed carbon sequestered to the deeper ocean by the biological  
867 pump that will impact air-sea CO<sub>2</sub> exchange. In addition, in terms of impacts up  
868 the food chain, EP may be a better metric than NPP. Friedland et al. (2012)  
869 demonstrated that there is no correlation between fishery yield and NPP at the  
870 global scale, but that there are strong correlations between fishery yield and  
871 several other variables including chlorophyll concentration, the pe-ratio, and EP.  
872 These three proxies all correlate with the fraction of primary production by large  
873 phytoplankton. In this context, the results presented here suggest large future  
874 declines in fishery yield across the high-latitude North Atlantic.

875 Laufkötter et al. (2015a) suggest a strong impact of temperature modification  
876 of phytoplankton growth rates and other ecosystem processes (including  
877 zooplankton growth and grazing rates) to infer a strong top-down grazing  
878 influence on the NPP response to climate change, noting that phytoplankton  
879 community growth rates appear to increase at low latitudes in some models,  
880 even as available nutrient concentrations decline. Several factors make it difficult  
881 to interpret their results and compare to our findings. Many of the key fluxes and  
882 fields needed to support their hypotheses were not available in the archived  
883 output from the CMIP5 models. They were forced to rely on estimated nutrient  
884 limitation factors and growth rates for the only the surface ocean in their analysis.  
885 Temperature warming is strongest at the surface (Figure 1S). Thus, their analysis  
886 may overestimate the temperature effects for the whole euphotic zone. They also  
887 present results based on diatom-specific nutrient limitation patterns, on the  
888 phytoplankton group with the largest changes in limitation factors, and on

Deleted: We suggest that

Deleted: may be a more

Deleted: proxy

Deleted: systems than changes to NPP

Deleted: s with climate

Deleted: and climate

Deleted: is also likely

Deleted: proxy

Deleted:

Deleted: show that

Deleted: The

Deleted: future

901 comparing total grazing with total NPP for some models (Figures 6-8, Laufkötter  
902 et al. 2015a). This may not be representative of the growth and/or community  
903 responses. At low latitudes the diatoms might show the biggest declines in  
904 growth due to nutrient limitation, but they may be only a small component of the  
905 community in many of the models (Figure 8). Under increasing nutrient stress,  
906 phytoplankton community growth rates may increase simply due to a declining  
907 contribution from diatoms, as the smaller phytoplankton will typically grow  
908 faster at low nutrient concentrations. Looking at total grazing rates compared to  
909 NPP cannot account for these community effects. We agree that temperature  
910 effects may be important in the NPP climate change response and that the  
911 temperature influence on phytoplankton growth and on the ecosystem  
912 processing of NPP that leads to export are highly uncertain (Laufkötter et al.  
913 2015a). Sherman et al. (2016) compiled in situ estimates of phytoplankton  
914 community growth rates at the global-scale, and found a relatively weak  
915 apparent temperature effect (apparent  $Q_{10} \sim 1.5$ ). The observational estimates of  
916 phytoplankton community growth rates were compared with the CESM and  
917 GFDL simulations analyzed here. ESMs used in climate change studies need to  
918 ensure that the emergent, apparent temperature-growth relation matches this  
919 observed value (even though higher explicit  $Q_{10}$  values may be prescribed for  
920 individual plankton functional types) to avoid biases in the response to  
921 temperature change (Sherman et al., 2016).

922 Many of the CMIP5 models have an assumed higher export efficiency for  
923 diatoms relative to small phytoplankton (Laufkötter et al., 2015b), building on a  
924 long-standing paradigm, strengthened by results from the detailed ecosystem  
925 studies of the Joint Global Flux Study (JGOFS) program (Boyd and Newton 1999;  
926 Buesseler 1998). In the current models, the spectrum of phytoplankton size

Deleted: much

928 structure is often represented very simply with only the end members of one  
929 large and one small phytoplankton group. Thus, the “diatom” group is a proxy  
930 for larger, efficiently-exporting, blooming phytoplankton functional types, DOM  
931 cycling, heterotrophic bacteria, microzooplankton, and the microbial loop are  
932 typically treated in an idealized, implicit manner in the current models as well.

Deleted: all the  
Deleted:  
Deleted:

933 To accurately predict the response of NPP and EP to climate change, it may  
934 be necessary to develop more robust ecosystem models with additional explicit  
935 phytoplankton, heterotrophic microbial, and zooplankton groups, including their  
936 impacts on nutrient cycling, export efficiency and the downward transport of  
937 organic matter. Models that include much greater diversity in the phytoplankton,  
938 show large community composition shifts with climate change (Dutkiewicz et al.  
939 2013). Quantifying the links between NPP, EP and community composition in  
940 observational datasets are a high priority. There are only limited field  
941 observations of the pe-ratio, some of which rely on nutrient drawdown and other  
942 indirect estimates of the sinking particle flux (Dunne et al. 2007). Further  
943 progress to improve model performance requires combined efforts from satellite,  
944 field, and laboratory observations, empirical and inverse modeling approaches,  
945 as well as process-based, forward models.

Deleted: Some m

Deleted: should be

Deleted: (Dunne et al., 2007)

946 The large model spread in EP and NPP, and significant biases seen in key  
947 nutrient fields for the 1990s suggest that the current ocean biogeochemical  
948 models are far from perfect and their results must be interpreted with some  
949 caution. However, the relationships between stratification and EP, NPP and  
950 nutrients do reveal some common mechanisms driving the climate change  
951 response. The large inter-model differences for the current era in NPP, EP and  
952 nutrient concentrations are partially associated with how these biogeochemical  
953 models are initialized and spun up for these experiments. The ocean

Deleted: is usually

960 biogeochemical models are often integrated in an offline mode for a thousand  
961 years or more before coupling to other components of the ESM (Séférian et al.,  
962 2016). The achieved preindustrial, near-steady state of biogeochemical fields may  
963 deviate substantially from the observed climatology, driven by biases in the  
964 physics and biogeochemistry. These differences typically persist in the present-  
965 day simulations and future projections. The advantage of the initialization and  
966 spin up process is that the biogeochemical fields are consistent with the  
967 simulated ocean circulation, and will respond to climate-driven changes  
968 appropriately. The strong intrinsic variability helps to reduce model drift and  
969 generate reasonable longer-term variability. As a result, these long-term  
970 simulations are suitable for analyzing climate trends, variability and sensitivities.  
971 RCP 8.5 is a strong warming scenario and the relationship between stratification  
972 changes and NPP/EP changes may be somewhat different under other RCP  
973 scenarios. Although the relations between the degree of surface warming and the  
974 ocean biogeochemical responses were largely linear across RCP 4.5 and 8.5 for  
975 the CESM(BGC) (Moore et al. 2013).

976 Some potentially important marine biogeochemical feedbacks on the climate  
977 system were missing completely or not well represented in the CMIP5 models,  
978 including important feedbacks through aerosol transport and deposition on the  
979 marine iron cycle, feedbacks involving the oxygen minimum zones and the  
980 marine nitrogen cycle, and the impacts on ocean biology by ongoing ocean  
981 acidification. Each of these feedbacks could impact phytoplankton and  
982 zooplankton community structures, NPP, EP, and pe-ratios in the future.

Deleted: the

983 It is also important to consider the longer-term climate change responses  
984 of both ocean physics and marine biogeochemistry. Moore et al. (2013) noted that  
985 climate impacts on the oceans were still accelerating at year 2100 under the RCP



Deleted: out

988 8.5 scenario (but not under the more moderate RCP 4.5 scenario). Randerson et al.  
989 (2015) extended the CESM1(BGC) RCP 8.5 scenario simulation examined here, to  
990 the year 2300. In these longer simulations, the climate impacts on ocean physical  
991 fields and biogeochemistry lead to even stronger perturbations after 2100 than  
992 those presented here for the 2090s. In addition, the ocean contribution to the  
993 climate-carbon feedback exceeded the land contribution after the year 2100  
994 (Randerson et al. 2015).

995

## 996 **5 Acknowledgments**

997 We are grateful for support from the U.S. Dept. of Energy Office of Science and  
998 the National Science Foundation (NSF). This contribution was supported by a grant to  
999 UCI as a part of the BGC Feedbacks Scientific Focus Area within the Regional and  
1000 Global Climate Modeling (RGCM) Program in the Climate and Environmental Sciences  
1001 Division (CESD) of the Biological and Environmental Research (BER) Program in the  
1002 US Dept. of Energy Office of Science. We also received funding from the NSF project  
1003 “Collaborative Research: Improved Regional and Decadal Predictions of the Carbon  
1004 Cycle“(AGS-1048890). We would also like to thank all those in the CMIP5 project  
1005 efforts, which made this work possible.

1006

1007

1009 **6 References**

1010 **Uncategorized References**

1011 [Alvain, S.; Moulin, C.; Dandonneau, Y.; Breon, F.M., 2005: Remote sensing of](#)  
1012 [phytoplankton groups in case 1 waters from global SeaWiFS imagery. \*Deep Sea\*](#)  
1013 [Res. Part I, 1, 1989–2004.](#)

1014 Aumont, O., and L. Bopp, 2006: Globalizing results from ocean in situ iron  
1015 fertilization studies. *Global Biogeochemical Cycles*, **20**.

1016 Azam, F., T. Fenchel, J. G. Field, J. S. Gray, L. A. Meyerreil, and F. Thingstad,  
1017 1983: The Ecological Role Of Water-Column Microbes In The Sea. *Marine Ecology*  
1018 *Progress Series*, **10**, 257-263.

1019 Behrenfeld, M. J., and Coauthors, 2006: Climate-driven trends in contemporary  
1020 ocean productivity. *Nature*, **444**, 752-755.

1021 Bentsen, M., and Coauthors, 2013: The Norwegian Earth System Model,  
1022 NorESM1-M - Part 1: Description and basic evaluation of the physical climate.  
1023 *Geoscientific Model Development*, **6**, 687-720.

1024 Bindoff, N. L., and Coauthors, 2007: Observations: oceanic climate change and  
1025 sea level. Cambridge University Press, 385-432.

1026 Bopp, L., O. Aumont, P. Cadule, S. Alvain, and M. Gehlen, 2005: Response of  
1027 diatoms distribution to global warming and potential implications: A global  
1028 model study. *Geophysical Research Letters*, **32**.

1029 Bopp, L., and Coauthors, 2001: Potential impact of climate change on marine  
1030 export production. *Global Biogeochemical Cycles*, **15**, 81-99.

1031 Bopp, L., and Coauthors, 2013: Multiple stressors of ocean ecosystems in the 21st  
1032 century: projections with CMIP5 models. *Biogeosciences*, **10**, 6225-6245.

1033 Boyd, P. W., and P. P. Newton, 1999: Does planktonic community structure  
1034 determine downward particulate organic carbon flux in different oceanic  
1035 provinces? *Deep-Sea Research Part I-Oceanographic Research Papers*, **46**, 63-91.

1036 [Bracegirdle, T. J., E. Shuckburgh, J.-B. Sallee, Z. Wang, A. J. S. Meijers, N.](#)  
1037 [Bruneau, T. Phillips, and L. J. Wilcox, 2013: Assessment of surface winds over the](#)  
1038 [Atlantic, Indian, and Pacific Ocean sectors of the SouthernOcean in](#)  
1039 [CMIP5models: historical bias, forcing response, and state dependence, J.](#)  
1040 [Geophys. Res. Atmos., 118, 547–562, doi:10.1002/jgrd.50153.](#)

1041 Buesseler, K. O., 1998: The decoupling of production and particulate export in  
1042 the surface ocean. *Global Biogeochemical Cycles*, **12**, 297-310.

1043 [Buitenhuis, E. T., T. Hashioka, and C. L. Quere, 2013a: Combined constraints on](#)  
1044 [global ocean primary production using observations and models, Global](#)  
1045 [Biogeochem. Cycles, 27, 847–858, doi:10.1002/gbc.20074.](#)

1046 Buitenhuis, E., and Coauthors, 2013b: MAREDAT: towards a world atlas of  
1047 MARine Ecosystem DATA. *Earth System Science Data*, **5**, 227-239.

1048 Cabré, A., I. Marinov, and S. Leung, 2015: Consistent global responses of marine  
1049 ecosystems to future climate change across the IPCC AR5 earth system models.  
1050 *Climate Dynamics*, **45**, 1253-1280.

1051 Capotondi, A., M. A. Alexander, N. A. Bond, E. N. Curchitser, and J. D. Scott,  
1052 2012: Enhanced upper ocean stratification with climate change in the CMIP3  
1053 models. *Journal of Geophysical Research-Oceans*, **117**.

1054 Carr, M.-E., and Coauthors, 2006: A comparison of global estimates of marine  
1055 primary production from ocean color. *Deep-Sea Research Part Ii-Topical Studies in*  
1056 *Oceanography*, **53**, 741-770.

1057 [Cheng, W., Chiang, J.C.H., and D. Zhang, 2013: Atlantic meridional overturning](#)  
1058 [circulation \(AMOC\) in CMIP5 model: RCP and Historical simulations. J. Climate,](#)  
1059 [26: 7187-7197, doi: 10.1175/JCLI-D-12-00496.](#)

1060 Collins, W. J., and Coauthors, 2011: Development and evaluation of an Earth-  
1061 System model-HadGEM2. *Geoscientific Model Development*, **4**, 1051-1075.

1062 Dufresne, J. L., and Coauthors, 2013: Climate change projections using the IPSL-  
1063 CM5 Earth System Model: from CMIP3 to CMIP5. *Climate Dynamics*, **40**, 2123-  
1064 2165.

1065 Dugdale, R. C., and J. J. Goering, 1967: Uptake of new and regenerated forms of  
1066 nitrogen in primary productivity. *Limnology and Oceanography*, **12**, 196-206.

1067 Dunne, J. P., J. L. Sarmiento, and A. Gnanadesikan, 2007: A synthesis of global  
1068 particle export from the surface ocean and cycling through the ocean interior and  
1069 on the seafloor. *Global Biogeochemical Cycles*, **21**.

1070 Dunne, J. P., and Coauthors, 2013: GFDL's ESM2 Global Coupled Climate-  
1071 Carbon Earth System Models. Part II: Carbon System Formulation and Baseline  
1072 Simulation Characteristics. *J Climate*, **26**, 2247-2267.

1073 Dunne, J. P., and Coauthors, 2012: GFDL's ESM2 Global Coupled Climate-  
1074 Carbon Earth System Models. Part I: Physical Formulation and Baseline  
1075 Simulation Characteristics. *J Climate*, **25**, 6646-6665.

1076 Dutkiewicz, S., J. R. Scott, and M. J. Follows, 2013: Winners and losers: Ecological  
1077 and biogeochemical changes in a warming ocean. *Global Biogeochemical Cycles*, **27**,  
1078 463-477.

1079 Eppley, R. W., and B. J. Peterson, 1979: Particulate Organic-Matter Flux And  
1080 Planktonic New Production In The Deep Ocean. *Nature*, **282**, 677-680.

1081 Friedland, K. D., and Coauthors, 2012: Pathways between primary production  
1082 and fisheries yields of large marine ecosystems. *PLoS One*, **7**, e28945.

1083 Froelicher, T. L., F. Joos, G. K. Plattner, M. Steinacher, and S. C. Doney, 2009:  
1084 Natural variability and anthropogenic trends in oceanic oxygen in a coupled  
1085 carbon cycle-climate model ensemble. *Global Biogeochemical Cycles*, **23**.

1086 Fung, I. Y., S. C. Doney, K. Lindsay, and J. John, 2005: Evolution of carbon sinks  
1087 in a changing climate. *Proceedings of the National Academy of Sciences of the United*  
1088 *States of America*, **102**, 11201-11206.

1089 [Garcia, H. E., R. A. Locarnini, M. M. Zweng, O. K. Baranova, and D. R. Johnson,](#)  
1090 [2010. Nutrients \(Phosphate, Nitrate, Silicate\). Vol. 4, World Ocean Atlas 2009,](#)  
1091 [NOAA Atlas NESDIS 71,398 pp.](#)

1092 Gent, P. R., and Coauthors, 2011: The Community Climate System Model  
1093 Version 4. *J Climate*, **24**, 4973-4991.

1094 Giorgetta, M. A., and Coauthors, 2013: Climate and carbon cycle changes from  
1095 1850 to 2100 in MPI - ESM simulations for the Coupled Model Intercomparison  
1096 Project phase 5. *Journal of Advances in Modeling Earth Systems*, **5**, 572-597.

1097 Goldstein, B., F. Joos, and T. F. Stocker, 2003: A modeling study of oceanic  
1098 nitrous oxide during the Younger Dryas cold period. *Geophysical Research Letters*,  
1099 **30**.

1100 [Bracegirdle, T. J., E. Shuckburgh, J.-B. Sallee, Z. Wang, A. J. S. Meijers, N.](#)  
1101 [Bruneau, T. Phillips, and L. J. Wilcox, 2013: Assessment of surface winds over the](#)  
1102 [Atlantic, Indian, and Pacific Ocean sectors of the Southern Ocean in](#)  
1103 [CMIP5 models: historical bias, forcing response, and state dependence, J.](#)  
1104 [Geophys. Res. Atmos., 118, 547–562, doi:10.1002/jgrd.50153.](#)

1105 Hannon, E., P. W. Boyd, M. Silviso, and C. Lancelot, 2001: Modeling the bloom  
1106 evolution and carbon flows during SOIREE: Implications for future in situ iron-  
1107 enrichments in the Southern Ocean. *Deep-Sea Research Part II-Topical Studies in*  
1108 *Oceanography*, **48**, 2745-2773.

1109 [Hauck, J., et al. \(2015\), On the Southern Ocean CO2 uptake and the role of the](#)  
1110 [biological carbon pump in the 21st century, Global Biogeochem. Cycles, 29, 1451–](#)  
1111 [1470, doi:10.1002/2015GB005140](#)

1112 [Hirata, T.; Hardman-Mountford, N.J.; Brewin, R.J.W.; Aiken, J.; Barlow, R.;](#)  
1113 [Suzuki, K.; Isada, T.; Howell, E.; Hashioka, T.; Aita-Noguchi, M.; et al., 2008:](#)  
1114 [Synoptic relationships between surface Chlorophyll-a and diagnostic pigments](#)  
1115 [specific to phytoplankton functional types. Biogeosciences, 8, 311–327.](#)

1116 Ilyina, T., K. D. Six, J. Segschneider, E. Maier - Reimer, H. Li, and I. Núñez -  
1117 Riboni, 2013: Global ocean biogeochemistry model HAMOCC: Model  
1118 architecture and performance as component of the MPI - Earth system model in  
1119 different CMIP5 experimental realizations. *Journal of Advances in Modeling Earth*  
1120 *Systems*, **5**, 287-315.

1121 [Ito, T., A. Bracco, C. Deutsch, H. Frenzel, M. Long, and Y. Takano \(2015\),](#)  
1122 [Sustained growth of the Southern Ocean carbon storage in a warming climate,](#)  
1123 [Geophys. Res. Lett., 42, 4516–4522, doi:10.1002/2015GL064320.](#)

1124 [Kostadinov, T.S.; Siegel, D.A.; Maritorena, S., 2009: Retrieval of the particle size](#)  
1125 [distribution from satellite ocean color observations. \*J. Geophys. Res.\*, \*114\*, C09015.](#)

1126 Jin, X., N. Gruber, J. P. Dunne, J. L. Sarmiento, and R. A. Armstrong, 2006:  
1127 Diagnosing the contribution of phytoplankton functional groups to the  
1128 production and export of particulate organic carbon, CaCO<sub>3</sub>, and opal from  
1129 global nutrient and alkalinity distributions. *Global Biogeochemical Cycles*, **20**.

1130 Jones, C., and Coauthors, 2011: The HadGEM2-ES implementation of CMIP5  
1131 centennial simulations. *Geoscientific Model Development*, **4**, 543-570.

1132 Knutti, R., and G. C. Hegerl, 2008: The equilibrium sensitivity of the Earth's  
1133 temperature to radiation changes. *Nature Geoscience*, **1**, 735-743.

1134 Kuhlbrodt, T., and J. M. Gregory, 2012: Ocean heat uptake and its consequences  
1135 for the magnitude of sea level rise and climate change. *Geophysical Research Letters*,  
1136 **39**.

1137 [Laufkötter, C., Vogt, M., Gruber, N., Aumont, O., Bopp, L., Doney, S. C., Dunne,](#)  
1138 [J. P., Hauck, J., John, J. G., Lima, I. D., Seferian, R., and Völker, C., 2015: Projected](#)  
1139 [decreases in future marine export production: the role of the carbon flux through](#)  
1140 [the upper ocean ecosystem, \*Biogeosciences Discuss.\*, \*12\*, 19941-19998,](#)  
1141 [doi:10.5194/bgd-12-19941-2015.](#)

1142 [Laufkötter, C., Vogt, M., Gruber, N., Aita-Noguchi, M., Aumont, O., Bopp, L.,](#)  
1143 [Buitenhuis, E., Doney, S. C., Dunne, J., Hashioka, T., Hauck, J., Hirata, T., John, J.,](#)  
1144 [Le Quéré, C., Lima, I. D., Nakano, H., Seferian, R., Totterdell, I., Vichi, M., and](#)  
1145 [Völker, C., 2015: Drivers and uncertainties of future global marine primary](#)  
1146 [production in marine ecosystem models, \*Biogeosciences\*, 12, 6955-6984,](#)  
1147 [doi:10.5194/bg-12-6955-2015.](#)

1148 Le Quere, C., and Coauthors, 2005: Ecosystem dynamics based on plankton  
1149 functional types for global ocean biogeochemistry models. *Global Change Biology*,  
1150 **11**, 2016-2040.

1151 [Leung, S., Cabré, A., and I. Marinov, 2015: A latitudinally banded phytoplankton](#)  
1152 [response to 21st century climate change in the Southern Ocean across the CMIP5](#)  
1153 [model suite. \*Biogeosciences\*, 12, 5715–5734, doi:10.5194/bg-12-5715-2015.](#)

1154 Liu, M., and Coauthors, 2014: What is the importance of climate model bias when  
1155 projecting the impacts of climate change on land surface processes? *Biogeosciences*,  
1156 **11**, 2601-2622.

1157 Luo, Y. Y., Q. Y. Liu, and L. M. Rothstein, 2009: Simulated response of North  
1158 Pacific Mode Waters to global warming. *Geophysical Research Letters*, **36**.

1159 Lyman, J. M., and Coauthors, 2010: Robust warming of the global upper ocean.  
1160 *Nature*, **465**, 334-337.

1161 Manizza, M., C. Le Quere, A. J. Watson, and E. T. Buitenhuis, 2008: Ocean  
1162 biogeochemical response to phytoplankton-light feedback in a global model.  
1163 *Journal of Geophysical Research-Oceans*, **113**.

1164 Marinov, I., S. C. Doney, I. D. Lima, K. Lindsay, J. K. Moore, and N. Mahowald,  
1165 2013: North-South asymmetry in the modeled phytoplankton community  
1166 response to climate change over the 21st century. *Global Biogeochemical Cycles*, **27**,  
1167 1274-1290.

Formatted: Font:Not Bold

Formatted: Font:Not Bold

1168 Misumi, K., K. Lindsay, J. Moore, S. Doney, F. Bryan, D. Tsumune, and Y.  
1169 Yoshida, 2014: The iron budget in ocean surface waters in the 20th and 21st  
1170 centuries: projections by the Community Earth System Model version 1.  
1171 *Biogeosciences*, **11**, 33-55.

1172 Moore, J., K. Lindsay, S. Doney, M. Long, and K. Misumi, 2013: Marine  
1173 Ecosystem Dynamics and Biogeochemical Cycling in the Community Earth  
1174 System Model [CESM1(BGC)]: Comparison of the 1990s with the 2090s under the  
1175 RCP4.5 and RCP8.5 Scenarios. *J Climate*, **26**, 9291-9312.

1176 Moore, J. K., S. C. Doney, and K. Lindsay, 2004: Upper ocean ecosystem  
1177 dynamics and iron cycling in a global three-dimensional model. *Global*  
1178 *Biogeochemical Cycles*, **18**, n/a-n/a.

1179 Moss, R. H., and Coauthors, 2010: The next generation of scenarios for climate  
1180 change research and assessment. *Nature*, **463**, 747-756.

1181 Pahlow, M., and U. Riebesell, 2000: Temporal trends in deep ocean Redfield  
1182 ratios. *Science*, **287**, 831-833.

1183 Passow, U., and C. A. Carlson, 2012: The biological pump in a high CO2 world.  
1184 *Marine Ecology Progress Series*, **470**, 249-271.

1185 Plattner, G. K., F. Joos, T. F. Stocker, and O. Marchal, 2001: Feedback mechanisms  
1186 and sensitivities of ocean carbon uptake under global warming. *Tellus Series B-*  
1187 *Chemical and Physical Meteorology*, **53**, 564-592.

1188 Pollard, R. T., and Coauthors, 2009: Southern Ocean deep-water carbon export  
1189 enhanced by natural iron fertilization. *Nature*, **457**, 577-U581.

1190 Pomeroy, L. R., 1974: The ocean's food web, a changing paradigm. *Bioscience*, **24**,  
1191 499-504.

1192 [Randerson, J. T., K. Lindsay, E. Munoz, W. Fu, J. K. Moore, F. M. Hoffman, N. M.](#)  
1193 [Mahowald, and S. C. Doney \(2015\), Multicentury changes in ocean and land](#)



1194 [contributions to the climate-carbon feedback, Global Biogeochem. Cycles,](#)  
1195 [29,doi:10.1002/2014GB005079.](#)  
1196 [Sallée, J.-B., E. Shuckburgh, N. Bruneau, A. J. S. Meijers, T. J. Bracegirdle, Z.](#)  
1197 [Wang, and T. Roy, 2013: Assessment of Southern Ocean water mass circulation](#)  
1198 [and characteristics in CMIP5 models: Historical bias and forcing response, \*J.\*](#)  
1199 [Geophys. Res. Oceans, 118, 1830–1844, doi:10.1002/jgrc.20135.](#)  
1200 Schmittner, A., and E. D. Galbraith, 2008: Glacial greenhouse-gas fluctuations  
1201 controlled by ocean circulation changes. *Nature*, **456**, 373-376.  
1202 Schmittner, A., A. Oschlies, H. D. Matthews, and E. D. Galbraith, 2008: Future  
1203 changes in climate, ocean circulation, ecosystems, and biogeochemical cycling  
1204 simulated for a business-as-usual CO2 emission scenario until year 4000 AD.  
1205 *Global Biogeochemical Cycles*, **22**.  
1206 [Séférian, R., and Coauthors, 2013: Skill assessment of three earth system models](#)  
1207 [with common marine biogeochemistry. \*Climate Dynamics\*, \*\*40\*\*, 2549-2573.](#)  
1208 [Séférian, R., M. Gehlen, L. Bopp, L. Resplandy, J. C. Orr<sup>2</sup>, O. Marti,](#)  
1209 [J. P. Dunne, J. R. Christian, S. C. Doney, T. Ilyina, K. Lindsay, P. Halloran,](#)  
1210 [C. Heinze, J. Segsneider, and J. Tjiputra, 2015: Inconsistent strategies to spin up](#)  
1211 [models in CMIP5: implications for ocean biogeochemical model performance](#)  
1212 [assessment. \*Geosci. Model Dev. Discuss.\*, \*\*8\*\*, 8751–8808. doi:10.5194/gmdd-8-8751-](#)  
1213 [2015.](#)  
1214 [Sherman, E., J. K. Moore, F. Primeau, and D. Tanouye, 2016: Temperature](#)  
1215 [influence on phytoplankton community growth rates, Global Biogeochem.](#)  
1216 [Cycles, 30, doi:10.1002/2015GB005272.](#)  
1217 [Siegel, D. A., K. O. Buesseler, S. C. Doney, S. F. Sailley, M. J. Behrenfeld, and P. W.](#)  
1218 [Boyd, 2014: Global assessment of ocean carbon export by combining satellite](#)  
1219 [observations and food-web models, Global Biogeochem. Cycles, 28,](#)  
1220 [doi:10.1002/2013GB004743.](#)

**Deleted:** Randerson, J., and Coauthors, 2015: Multi - century changes in ocean and land contributions to climate - carbon feedbacks. *Global Biogeochemical Cycles*, (in print).

**Deleted:** e

**Deleted:** e

**Formatted:** Font:Not Bold

**Formatted:** Font:Not Bold

**Formatted:** Font:Not Bold

**Formatted:** Font:Not Bold

**Formatted:** Font:Not Bold

**Formatted:** Font:Not Bold

**Formatted:** Font:Not Bold

1226 Siegenthaler, U., and T. Wenk, 1984: Rapid Atmospheric Co<sub>2</sub> Variations And  
1227 Ocean Circulation. *Nature*, **308**, 624-626.

1228 Steinacher, M., F. Joos, T. L. Froelicher, G. K. Plattner, and S. C. Doney, 2009:  
1229 Imminent ocean acidification in the Arctic projected with the NCAR global  
1230 coupled carbon cycle-climate model. *Biogeosciences*, **6**, 515-533.

1231 Steinacher, M., and Coauthors, 2010: Projected 21st century decrease in marine  
1232 productivity: a multi-model analysis. *Biogeosciences*, **7**, 979-1005.

1233 Swart, N. C., and J. C. Fyfe, 2012: Observed and simulated changes in the  
1234 Southern Hemisphere surface westerly wind-stress. *Geophysical Research Letters*,  
1235 **39**.

1236 Szopa, S., and Coauthors, 2013: Aerosol and ozone changes as forcing for climate  
1237 evolution between 1850 and 2100. *Climate Dynamics*, **40**, 2223-2250.

1238 Taylor, K. E., R. J. Stouffer, and G. A. Meehl, 2012: An Overview Of Cmp5 And  
1239 The Experiment Design. *Bulletin of the American Meteorological Society*, **93**, 485-498.

1240 Tjiputra, J. F., and Coauthors, 2013: Evaluation of the carbon cycle components in  
1241 the Norwegian Earth System Model (NorESM). *Geoscientific Model Development*, **6**,  
1242 301-325.

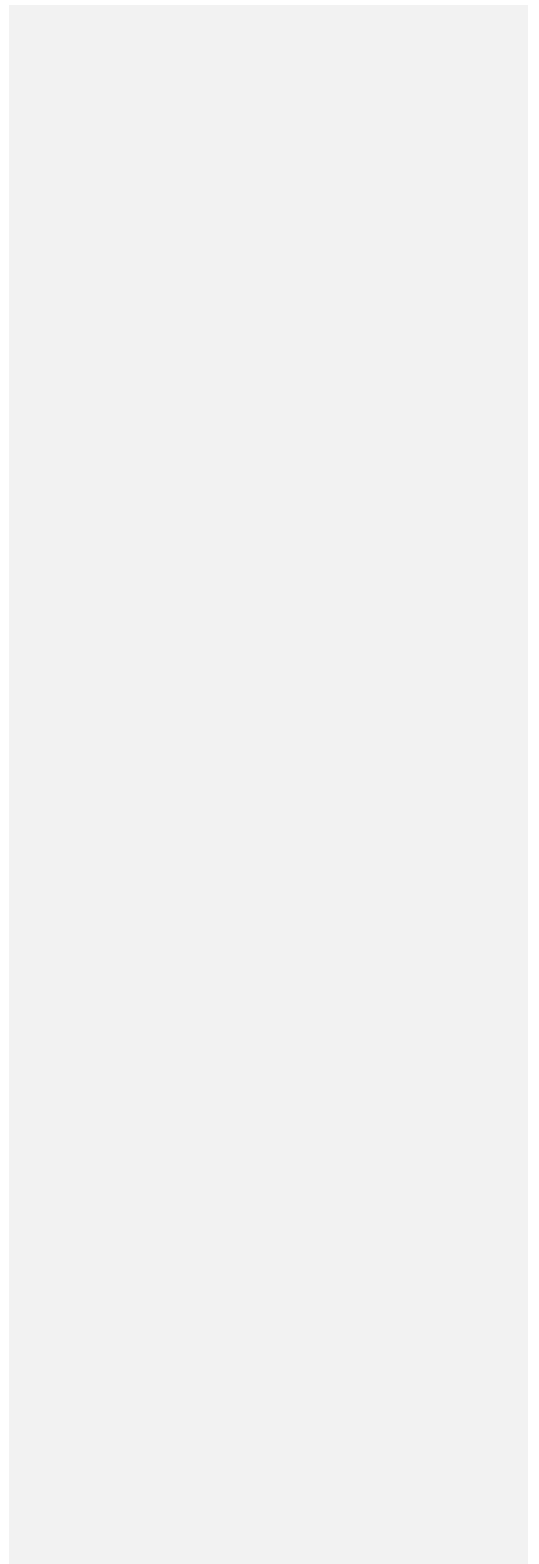
1243 van Vuuren, D. P., and Coauthors, 2011: The representative concentration  
1244 pathways: an overview. *Climatic Change*, **109**, 5-31.

1245 Vancoppenolle, M., L. Bopp, G. Madec, J. Dunne, T. Ilyina, P. R. Halloran, and N.  
1246 Steiner, 2013: Future Arctic Ocean primary productivity from CMIP5 simulations:  
1247 Uncertain outcome, but consistent mechanisms. *Global Biogeochemical Cycles*, **27**,  
1248 605-619.

1249 Vichi, M., and Coauthors, 2011: Global and regional ocean carbon uptake and  
1250 climate change: sensitivity to a substantial mitigation scenario. *Climate Dynamics*,  
1251 **37**, 1929-1947.

1252

1253



1254 **Figure Captions**

1255

1256 **Figure 1.** Time series of global mean surface stratification, SST and SSS for  
1257 historical run and RCP8.5 over 1850-2100. Surface stratification is defined as the  
1258 density difference between 200m and the surface. Red square indicates  
1259 observations from the WOA2009 data.

1260

1261 **Figure 2.** The spatial pattern for changes in stratification intensity changes  
1262 between the 1990s and the 2090s.

1263

1264 **Figure 3.** Time series of nitrate (NO<sub>3</sub>), phosphate (PO<sub>4</sub>), silicate (SiO<sub>4</sub>) and  
1265 dissolved iron (dFe) concentrations (0-100 m) are shown for 1850-2100. Red  
1266 square indicates WOA2009 global mean values.

1267

1268 **Figure 4.** Time series are displayed of mean changes (in percent) relative to the  
1269 1990s for (a) NO<sub>3</sub>, (b) PO<sub>4</sub>, (c) SiO<sub>4</sub> and (d) dFe (0-100m) during 1850-2100.

1270

1271 **Figure 5.** Time series of global mean net primary production, export production,  
1272 and the particle export ratio over 1850-2100 are shown for each model.

1273

1274 **Figure 6.** Time series are displayed of the percent changes in net primary  
1275 production, export production, and the particle export ratio, and stratification  
1276 over the period 1850-2100 (each relative to their 1990s means).

1277

1278 **Figure 7.** Relationships are shown between the relative percent change in surface  
1279 stratification with climate and the relative change in several biogeochemical  
1280 variables including net primary production (NPP) (a), silicate (b), nitrate (c),  
1281 phosphate (d), export production (EP) (e), the fraction of NPP by diatoms (g). EP  
1282 is plotted against the change in the fraction of NPP by diatoms (g) and against  
1283 the change in NPP (h). All changes are relative to the 1990s and plotted over  
1284 1850-2100. These time series are derived from global annual mean data.

1285

1286 **Figure 8.** The fraction of total NPP by diatoms for the 1990s is shown for each  
1287 model (data for NorESM not available).

1288

1289 **Figure 9.** The percent change in NPP by diatoms between the 2090s and the 1990s.

1290

1291 **Figure 10.** The mean particle export ratio for the 1990s is shown for each model.

1292

**Deleted:** Figure 2. Mean vertical profiles are shown for density (a), temperature (c) and salinity (e) for the 1990s. Changes between the 2090s-1990s are shown in (b), (d) and (f), for the same variables. Solid black line denotes WOA2009 data.

**Deleted:** 4

**Deleted:** 5

**Deleted:** 6

**Deleted:** Figure 7. Mean NO<sub>3</sub> concentrations in the first 100 m for the 1990s, R-squared and logarithmic transformed root mean square error (RMSE) are indicated relative to observations from the WOA2009.

**Deleted:** 8

**Deleted:** 9

**Deleted:** 10

**Deleted:** 11

**Deleted:** 12

**Deleted:** 3

1312 Figure 11. The percent change in the particle export ratio (pe-ratio) between the  
1313 2090s and the 1990s).

Formatted: Font:Bold

1314  
1315 Figure 12. The stratification bias for the 1990s is plotted for each model versus  
1316 the relative changes in NPP (a), EP (b), and stratification (C) with climate change  
1317 (2090s – 1990s).

Deleted: 4

### 1318 1319 1320 Supplementary Figure Captions

Formatted: Font:Bold

1321  
1322 Figure S1. Mean vertical profiles are shown for density (a), temperature (c) and  
1323 salinity (e) for the 1990s. Changes between the 2090s-1990s are shown in (b), (d)  
1324 and (f), for the same variables. Solid black line denotes WOA2009 data.

1325  
1326 Figure S2. Fractional contribution of temperature to the stratification change  
1327 from the 1990s to the 2090s is shown for each model.

1328  
1329 Figure S3. Mean NO<sub>3</sub> concentrations in the first 100 m for the 1990s, R-squared  
1330 and logarithmic transformed root mean square error (RMSE) are indicated  
1331 relative to observations from the WOA2009.

1332  
1333

**Figure 2.** Mean vertical profiles are shown for density (a), temperature (c) and salinity (e) for the 1990s. Changes between the 2090s-1990s are shown in (b), (d) and (f), for the same variables. Solid black line denotes WOA2009 data.

**Figure 3.** Fractional contribution of temperature to the stratification change from the 1990s to the 2090s is shown for each model.

**Figure 7.** Mean  $\text{NO}_3$  concentrations in the first 100 m for the 1990s, R-squared and logarithmic transformed root mean square error (RMSE) are indicated relative to observations from the WOA2009.